ensor Planning for 3D Object earch [1]

by

Yiming Ye[1] and **John K. Tsotsos**[2]
IBM T. J. Watson Research Center[1], P.O. Box 704, Yorktown Heights, NY 10598, USA
Email: yiming@watson.ibm.com; Tel: (914) 784-7460; Fax: (914) 784-7455
Dept. of Computer Science, University of Toronto[2],Toronto Ontario, Canada M5S 1A4
Email: tsotsos@vis.toronto.edu; Tel: (416) 978-3619; FAX: 416-978-1455

[1]Published by: *Computer Vision and Image Understanding, Vol. 73, No. 2, February, pp. 145-168, 1999, Academic Press, Inc.*

Abstract

In this paper, we provide a systematic study of the task of sensor planning for object search. The search agent's knowledge of object location is encoded as a discrete probability density which is updated whenever a sensing action occurs. Each sensing action of the agent is defined by a viewpoint, a viewing direction, a field-of-view, and the application of a recognition algorithm. The formulation casts sensor planning as an optimization problem: the goal is to maximize the probability of detecting the target with minimum cost. This problem is proved to be NP-Complete, thus a heuristic strategy is favored. To port the theoretical framework to a real working system, we propose a sensor planning strategy for a robot equipped with a camera that can pan, tilt, and zoom. v ime,e e f posiobls actiosr

List of Symbols

a,b,c,d,e,f,g,h,i,j,k,l,m,n,o,p,q,r,s,t,u,v,w,x,y,z

A,B,C,D,E,F,G,H,I,J,K,L,M,N,O,P,Q,R,S,T,U,V,W,X,Y,Z

0,1,2,3,4,5,6,7,8,9,0

Ω, $\bigcup$, $\neq$, $\sum$, α, β, $\neg$, $\ldots$, $\prod$, $\bigcap$, $\bigcap$, $\times$, Δ, (,), [,], \{, \}, θ, δ, $>$, $<$,$\hat{;}$ $\emptyset$, σ, π

This work is supported by ARK project and IBM Centre for Advanced Studies. The authors would like to thank the anonymous reviewers and Chris Brown, Eugene Fiume, Eric Harley, Piotr Jasiobedzki, Allan Jepson, Victor Lee, Hector Levesque, Demetri Terzopoulos and Dave Wilkes for their valuable comments and help.

Contents

1 Introduction **1**

2 Overview **2**

3 Problem Formulation **5**

4 Detection Function **8**

5 Sensed Sphere **11**

6 Where to Look Next **13**
- 6.1 Determine the Necessary Viewing Angle Size 13
- 6.2 Determining the Necessary Viewing Directions for a Given Angle Size 16
- 6.3 Selecting the Next Action 18

7 Where to Move Next **19**
- 7.1 Selecting the Next Robot Position 19
- 7.2 The Solidity Property 21
- 7.3 When to Stop Searching 22

8 Testing the Model **22**
- 8.1 Simulated Environments 22
- 8.2 Real Environments 24

9 Conclusion **30**

A The Complexity of the Sensor Planning Task **31**

B Properties of the Greedy Strategy **33**

1 Introduction

The research described in this paper addresses the task of efficiently searching for a given 3D object in a given 3D environment by a mobile platform equipped with a camera and, if the environment configuration is not known, a method of calculating depth, like a stereo or laser range finder. It is clear that exhaustive, brute-force blind search will suffice for its solution; however, our goal is the design of efficient strategies for search because exhaustive search is computationally and mechanically prohibitive for non-trivial situations. In general, this task consists of three subtasks. The first subtask is the selection of the sensing parameters so as to bring the target into the field of view of the sensor with sufficient image quality that it can be detected by the recognition algorithms. This is called the sensor planning problem for object search, and it is the main concern of this paper. The second subtask is the manipulation of the hardware so that the sensing operators can reach the state specified by the planner. The recent availability of sophisticated hardware for sensor/platform control and real-time image processing makes this task feasible. The third subtask involves searching for the target within the image. This is the object recognition and localization problem, which attracts considerable attention within the computer vision community.

Sensor planning for object search is very important if a robot is to interact intelligently and effectively with its environment. For example, a robot often needs to use sensory information to determine the position of the objects in its workspace in order to manipulate them. It is generally impractical to determine the location of the object before it is needed. Because of the camera's limited field of view, occlusion, the limited depth of field of lenses, the lighting conditions and other factors, it is often necessary to obtain many images using many camera configurations and viewpoints (see [58] for further discussion). Also, a robot navigating in an industrial environment often needs to search the environment for known landmarks in order to estimate its own position. The above two examples illustrate the critical requirement for efficient directing of the sensor.

Object search has been examined in a variety of ways by the computer vision community ([51], [60], [19], [39], [44]). Garvey [19] proposes the idea of indirect search for the target: first the sensor is directed to search for an "intermediate" object that commonly participates in a spatial relationship with the target, and then the sensor is directed to examine the restricted region specified by this relationship. Wixson and Ballard [59] [60] present a mathematical model of search efficiency and analyze the efficiency of indirect search over a wide range of situations that vary the spatial structure of the domain as well as recognition performances. They conclude that indirect search can improve efficiency in many situations. Connell et al. [14] construct a robot that roams an area searching for and collecting soda cans. The robot is designed to follow the walls of the room and the sensor only searches the area immediately in front of the robot. This may not be very efficient since the likelihood target presence is not considered. It is interesting to note that the operational research community has extensively studied the problem of optimal search [31]. Their approach, however, is very general and sensor planning is not involved.

Object search is a task that is particularly well suited to the active vision approach. Thus the study of object search may produce results that will improve our understanding of certain aspects of an active vision system. For example, it may elucidate the role of a sensor planning component in a task oriented system and its relationship to the vision component. The active vision approach argues that rather than simply analyze a set of pre-recorded images, the observer should actively control its image acquisition process so that the acquired images be relevant and useful for the task at hand. Considering the efficiency of action selection, there are two extremes. At one end is Brooks's theory on reactive planning [12], in which no time is spent on calculating the action sequence. At the other end is the strategy of reconstructing every detail of the environment and then selecting an action sequence that is best according to given criteria. The goal of the sensor planning system is to find a balance between these extremes such that the task can be best performed within given limits on effort.

Previous research has generally placed much more emphasis on image analysis than on sensor planning. The sensor planning problem, however, is very important, since it is the sensor's state parameters which for the most part determine the quality of the resulting image. For some task oriented vision systems, e.g., object search, sensor planning is definitely required. Recently, more and more work on sensor planning for computer vision has appeared. For example, Krotkov[33][34] considers the problem of how to determine the focus motor position providing the sharpest focus on an object point at an unknown distance and how to compute the distance to a sharply focused object point. Cowan et al. [15] and Tarabanis et al. [47] present approaches to automatically generate the possible camera locations, orientations, and optical settings for observing an object.

There is also work on sensor planning with respect to task oriented systems. For example, Rimey and Brown [44] use composite Bayes net and utility decision rules to plan the sensor in their task-oriented system TEA. Grimson [55] proposes an optimal sensing strategy for disambiguating among alternative interpretations of scenes containing multiple polyhedral objects (multiple objects in known poses or a single object with several consistent poses). Hutchinson and Kak [24] implement a system that reasons about high-level operational goals, geometric goals, and uncertainty-reduction goals to create task plans for an assembly robot. Maver and Bajcsy [39] develop a strategy to determine the sequence of different views to check hidden regions by using a laser scanning system. Jensen, Christensen, and Nielsen [26] show how causal probabilistic networks together with Bayesian methods can be used for modeling contexts and for interpretation of image processing findings. Levitt, Agosta, and Binford [36] demonstrate an approach to automated control of vision systems through influence diagrams. Dickinson, Christensen, Tsotsos, and Olofesson [18] combine an attention mechanism and a viewpoint control strategy to perform active object recognition.

This paper provides the first formalization of the sensor planning task for object search and proposes a practical sensor planning strategy. Instead of examining different aspects of object search separately, our formulation emphasizes the relationship between action and image processing and integrates the two into a complete system. During sensor planning we decompose the huge space of possible sensing actions into a finite set of actions that must be considered. This greatly simplifies the sensor planning task. Simulation experiments and real experiments are presented to support the concept.

2 Overview

At first glance object search seems easy. But when we study the task more deeply, we find it is not so easy at all. In this section, we analyze the factors that influence the object search task and give an overview of our strategy.

The model of the search agent is based on the ARK robot (Figure 1(b)) [42], which is a mobile platform equipped with a special sensor: the Laser Eye [25] (Figure 1(a)). The Laser Eye is mounted on a robotic head with pan and tilt capabilities. It consists of a camera with controllable focal length (zoom), a laser range-finder and a mirror. The height of the camera is fixed. The mirror is used to ensure collinearity of effective optical axes of the camera lens and the range finder. With this mirror, the laser range finder can measure the distance from the center of the camera to the object along the camera viewing axis. The camera's image plane is assumed to be always coincident with its focal plane.

The task is to search for a target, such as a baseball, within an environment, such as the one described in Figure (13). The goal is to design an efficient strategy to find the target. Throughout

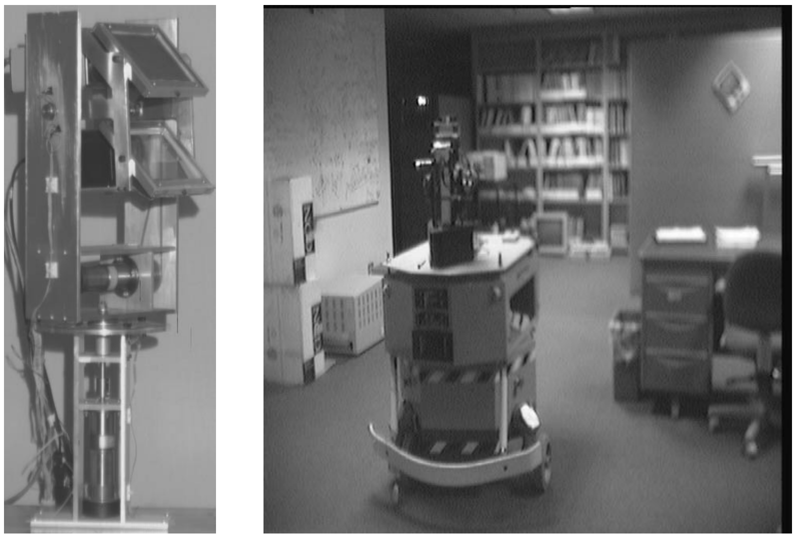
(a) (b)

Figure 1: The hardware used in the paper

(a) The Laser Eye. At the top is the Optech laser range finder, at the bottom is the zoom and focus controlled lens. The two mirrors are used to ensure collinearity of effective optical axes of the camera lens and the range finder. The pan-tilt unit is operated by two DC servocontrolled motors from Micromo Electronics, equipped with gearboxes and optical encoders. (b) The ARK mobile platform, which is a 3 *wheeled Cybermotion K2A platform equipped with a small number of sonar transducers.*

the paper, we assume that the target is not allowed to move and that the floor of the environment is flat. We assume that recognition algorithms for the given target only are available, and further, to simplify the discussion, that there is just one recognition algorithm.

Perhaps the most obvious search strategy that comes to mind is to perform a 360^o pan using only wide-angle settings. This might work in some situations, but not others. For example, this strategy might be effective when searching for a soccer ball within the environment depicted in Figure (13), but not when searching for a small battery. At the wide-angle setting the image of the battery might be too small to detect. Even when the wide-angle setting is appropriate for checking the environment, we still need to select the camera's viewing directions to perform the 360^o pan.

Thus, the first task is to decide upon the camera angle sizes which suffice for examining the environment. For a given camera angle size, the target can be detected only when it is within a certain range of distance (effective range) from the camera center (Figure 5). Our strategy, as described in Section 6.1, is to select a group of camera angle sizes such that no matter where the target is in the environment, one of them can make the image of the target good enough to be detected.

Each selected angle size can successfully examine a layer of the sphere surrounding the camera center (Figure 8). Therefore, the second task is to decide how to select the corresponding viewing directions to examine the given layer. In Section 6.2, we present an algorithm that selects a set of viewing directions that suffice to cover the corresponding layer. For each viewing direction we can successfully examine a portion of the spherical layer (called the effective volume) corresponding to the intersection of the layer and the wedge-shaped viewing volume associated with the camera's viewing direction.

For each camera angle size, we can select a group of viewing directions. The union of the camera parameter settings (determined by direction and angle size) of all the selected viewing angle sizes gives the total camera parameter settings that are needed to examine the whole environment. To search for the target, we only need to try these camera settings one by one. We call this strategy the "Non Planning" strategy. Suppose we have m settings, then the expected number of settings that need to be tried in order to find the target is:

$$\frac{1}{m} \times 1 + [(1-\frac{1}{m})]\frac{1}{m-1} \times 2 + \cdots + [(1-\frac{1}{m})\cdots(1-\frac{1}{1-(m-2)})]\frac{1}{m-1} \times m = \frac{m+1}{2} \qquad (1)$$

When m is large or the amount of time needed to analyze the image taken by the camera is large, the "Non Planning" strategy is not efficient for target detection. To reduce the number of images to be analyzed, we need to plan the order in which camera settings are applied. By applying the most promising settings first we can increase the probability of detecting the target at an early stage.

What information should be considered when selecting the best camera settings? Maybe it is helpful to examine how people perform the search task. $3D$ visual search is a task that is very common in our everyday life. Almost every search process is guided by our knowledge — we always search those regions that we believe most likely to contain the target. This illustrates that knowledge about possible positions of the target is a very important during the search process and it should be used to guide the search.

In order to use this knowledge, we encode it as a target probability distribution. In addition, we propose a concept called the detection function to capture the statistical regularity linking object recognition algorithm, target object, and viewpoint parameters. By combining the target distribution and detection function, we are able to calculate the probability of detecting the target for a given camera setting. This information allows us to select those imaging geometries which have the best potential for yielding useful results. We call this strategy the "planning strategy".

So far, there is a very important factor that has not been considered — occlusion. The number of camera settings to be tried can be further reduced by considering only those settings whose effective volumes are not fully occluded or are not outside of the environment. This is easy to do if the geometry of the environment is known. When the geometry is not known, we use the Laser Eye to ping the laser around and construct the "sensed sphere" (Figure 16) which gives the region that is not occluded with respect to the camera center. This sensed sphere is then used to further restrict the camera settings to be considered.

The above completes the description of our search strategy when the robot position is fixed. We call this the "where to look next" strategy. The next task is how to move the robot when it seems that the current position is not likely to find the target. For each possible next position, there is a region that can be checked without occlusion. Our strategy, as described in Section 7.1, is to move to a position whose unoccluded region has the highest probability of presence of the target (Figure 10 (d)(e)(f)). As a result, the robot tends to move to a high probability region during the search process.

As a summary, there are two characteristics of our approach. The first is the decomposition of the huge number of camera parameter settings allowed by the hardware into limited settings that must be considered. This greatly reduces the complexity of the "where to look next" task. The second is the emphasis on guidance through the agent's knowledge. The advantage of this is that for relatively good knowledge, the most promising actions tend to be selected first, as shown in Figure 15. The drawback is that when the agent's knowledge is too far from reality, the performance will decrease greatly as shown in Table 3. There are many ways to perform object search other than the one we propose. For example, if there exist recognition algorithms that can detect other objects in addition to the target, then the indirect search strategy can greatly increase the search efficiency as illustrated by Wixson and Ballard [59].

3 Problem Formulation

In order to reveal basic insights into the structure of object search task and delimit the space of permissible solutions, we formulate the task and study it in a formal and theoretical fashion. We first define some basic concepts used in the discussion, then pinpoint the complexity of the task and propose a practical strategy to perform the task.

The search region Ω can be of any form, and it is assumed that we know the boundary of Ω exactly, although we do not know its internal configuration. In practice, we tessellate the region Ω into a series of elements c_i, $\Omega = \bigcup_{i=1}^{n} c_i$ and $c_i \bigcap c_j = 0$ for $i \neq j$. In the rest of the paper, we assume the search region is an office-like environment, and we tessellate the space into little cubes of equal size.

The model of the search agent, as described in Section 2, is a robot equipped with a pan, tilt, and zoom camera. There are three coordinate systems used to describe the geometric configuration of the search agent (Figure 2): the world coordinate system (WCS), the robot coordinate system (RCS) and the camera coordinate system (CCS). The WCS is fixed and corresponds to the search region Ω. The RCS is attached to the robot head with its origin at the center of the robot head. The direction of the RCS is the same as that of the WCS. The CCS corresponds to the camera and has its origin at the nodal point of the camera. Here we assume the origin of the CCS and the origin of the RCS are the same. The direction of the Z axis of the CCS is the same as the direction of the view axis of the camera. The direction of the X axis of the CCS is parallel to the horizontal direction of the image plane. The direction of the Y axis of the CCS is parallel to the vertical direction of the image plane. The direction of the camera viewing axis Z can be specified by the pan and tilt (p,t) with respect to the RCS. The pan p is the amount of counterclockwise rotation needed to bring the viewing axis of the camera into the XZ plane of the RCS; tilt t is the angle between the viewing axis of the camera and the Z axis of the RCS. The range for p and t are $0 \leq p < 2\pi$ and $0 \leq t < \pi$.

The state of the search agent is uniquely determined by 7 parameters $(x_c, y_c, z_c, w, h, p, t)$, where (x_c, y_c, z_c) is the position of the camera center in WCS, w and h are the solid angle width and solid angle height of the solid viewing angle of the camera. The position (x_c, y_c, z_c) can be adjusted by moving the mobile platform. The viewing angle size $<w, h>$ can be adjusted by the zoom lens of the camera. Pan and tilt (p,t) can be adjusted by the motors on the robotics head.

An operation $\mathbf{f} = \mathbf{f}(x_c, y_c, z_c, p, t, w, h, a)$ is an action of the searcher within the region Ω, where a is the recognition algorithm used to detect the target. An operation $\mathbf{f}$ entails two steps: (1) take a **perspective** projection image according to the camera configuration of $\mathbf{f}$, and then (2) search the image using the recognition algorithm a.

The target distribution can be specified by a probability distribution function $\mathbf{p}$. The term $\mathbf{p}(c_i, \tau)$ gives the probability that the center of the target is within cube c_i at time τ. Usually this distribution is assumed to be known at the beginning of the search process, and it is determined by our knowledge of the world. If we know nothing about the target probability distribution, then we can assume a uniform distribution at the beginning. Note, we use $\mathbf{p}(c_o, \tau)$ to represent the probability that the target is outside the search region at time τ. The following constraint holds

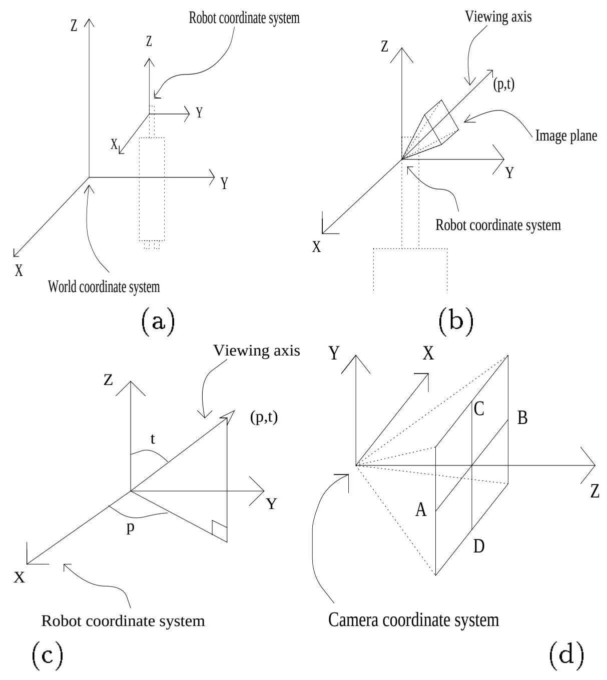

Figure 2: (a) The world coordinate system and the robot coordinate system; (b) The robot coordinate system and the camera viewing volume; (c) The robot coordinate system and the camera viewing axis direction (p, t). (d) The camera coordinate system and the image plane.

throughout the search process:

$$\mathbf{p}(c_o, \tau) + \sum_{i=1}^{n} p(c_i, \tau) = 1 \tag{2}$$

The detection function on Ω is a function $\mathbf{b}$, such that $\mathbf{b}(c_i, \mathbf{f})$ gives the conditional probability of detecting the target given that the center of the target is located within c_i, and the operation is $\mathbf{f}$. This function is further simplified as the conditional probability of detecting the target when the target center is located at the center of c_i. For any operation, if the projection of the center of the cube c_i is outside the image, we assume $\mathbf{b}(c_i, \mathbf{f}) = 0$; if the cube is occluded or too far from the camera or too near, we also have $\mathbf{b}(c_i, \mathbf{f}) = 0$. In general [61] [62], $\mathbf{b}(c_i, \mathbf{f})$ is determined by various factors, such as intensity, occlusion, and orientation, etc. It is obvious that the probability of detecting the target by applying action $\mathbf{f}$ is given by

$$P(\mathbf{f}) = \sum_{i=1}^{n} \mathbf{p}(c_i, \tau_{\mathbf{f}})\mathbf{b}(c_i, \mathbf{f}) \tag{3}$$

where $\tau_{\mathbf{f}}$ is the time just before $\mathbf{f}$ is applied. Let Ψ be the set of all the cubes that are within the field of view of $\mathbf{f}$ and that are not occluded, then we have

$$P(\mathbf{f}) = \sum_{c \in \Psi} \mathbf{p}(c, \tau_{\mathbf{f}})\mathbf{b}(c, \mathbf{f}) \tag{4}$$

The reason that the term $\tau_{\mathbf{f}}$ is introduced in the calculation of $P(\mathbf{f})$ is that the probability distribution needs to be updated whenever an action fails. Here we use Bayes' formula. Let α_i be the event that the center of the target is in cube c_i, and α_o be the event that the center of the target is outside the search region. Let β be the event that after applying a recognition action, the recognizer successfully detects the target. Then $P(\neg\beta \mid \alpha_i) = 1 - \mathbf{b}(c_i, \mathbf{f})$ and $P(\alpha_i \mid \neg\beta) = \mathbf{p}(c_i, \tau_{\mathbf{f}+})$, where $\tau_{\mathbf{f}+}$ is the time after $\mathbf{f}$ is applied. Since the above events $\alpha_1, \ldots, \alpha_n, \alpha_o$ are mutually complementary and exclusive, we get the following update rule

$$\mathbf{p}(c_i, \tau_{\mathbf{f}+}) = \frac{\mathbf{p}(c_i, \tau_{\mathbf{f}})(1 - \mathbf{b}(c_i, \mathbf{f}))}{\mathbf{p}(c_o, \tau_{\mathbf{f}}) + \sum_{j=1}^{n} \mathbf{p}(c_j, \tau_{\mathbf{f}})(1 - \mathbf{b}(c_j, \mathbf{f}))} \tag{5}$$

where $i = 1, \ldots, n, o$.

The cost $\mathbf{t_o}(\mathbf{f})$ gives the total time needed to (1)manipulate the hardware to the status specified by $\mathbf{f}$; (2)take a picture; (3)update the environment and register the space; and (4) run the recognition algorithm. We assume that: (2) and (3) are same for all the actions; (4) is known for any recognition algorithm and is constant for a given recognition algorithm.

Let $\mathbf{O_\Omega}$ be the set of all possible operations that can be applied. The effort allocation $\mathbf{F} = \{\mathbf{f}_1, \ldots, \mathbf{f}_k\}$ gives the ordered set of operations applied in the search, where $\mathbf{f}_i \in \mathbf{O_\Omega}$. $P(\mathbf{f}_1)$ gives the probability that the first action detects the target. $[1 - P(\mathbf{f}_1)]P(\mathbf{f}_2)$ gives the probability that the first action does not detect the target, but the second action detects the target. Similar analysis can be applied to other actions in $\mathbf{F}$. Finally, $\{\prod_{i=1}^{k-1}[1 - P(\mathbf{f}_i)]\}P(\mathbf{f}_k)$ gives the probability that $\mathbf{f}_1$, ..., $\mathbf{f}_{k-1}$ failed to detect the target, but $\mathbf{f}_k$ detects the target. It is clear that the probability of detecting the target by effort allocation $\mathbf{F}$ is given by:

$$P[\mathbf{F}] = P(\mathbf{f}_1) + [1 - P(\mathbf{f}_1)]P(\mathbf{f}_2) + \ldots + \{\prod_{i=1}^{k-1}[1 - P(\mathbf{f}_i)]\}P(\mathbf{f}_k) \tag{6}$$

The total cost for applying this allocation is (following [52]):

$$T[\mathbf{F}] = \sum_{i=1}^{k} \mathbf{t_o}(\mathbf{f}_i) \tag{7}$$

Suppose K is the total time that can be allowed in the search, then the task of sensor planning for object search can be defined as finding an allocation $\mathbf{F} \subset \mathbf{O_\Omega}$, which satisfies $T(\mathbf{F}) \leq K$ and maximizes $P[\mathbf{F}]$.

After some analyzes and manipulations, we have obtained many interesting properties and proved that sensor planning task for object search is NP complete (refer to Appendix A for properties).

Since the sensor planning problem is NP-complete and usually the number of the available candidate actions is large, it is necessary to simplify the original problem. Instead of looking for an algorithm that always generates an optimal solution, we simply use heuristics that will generate a feasible solution for the original problem. Here, we use a greedy strategy. The greedy method suggests that one can devise an algorithm which works in stages, considering one input at a time. At each stage, based on some optimization measure, the next candidate is selected and is included into the partial solution developed so far. Suppose we have already executed q ($q \geq 1$) actions $\mathbf{F}_q = \{\mathbf{f}_1, \ldots, \mathbf{f}_q\}$. We now want to find the next action $\mathbf{f}_{q+1}$ to execute, with the hope that our strategy of finding the next action may lead to an **approximate** solution for the object search task.

When we execute a next action $\mathbf{f}$, the effort allocation becomes $\mathbf{F}_{q+1} = \{\mathbf{f}_1, \ldots, \mathbf{f}_q, \mathbf{f}\}$. The expected probability of detecting the target is $P[\mathbf{F}_{q+1}] = P[\mathbf{F}_q] + \Delta_P(\mathbf{f})$, where $\Delta_P(\mathbf{f}) = \{\prod_{j=1}^{q}[1 - \sum_{i=1}^{n} \mathbf{p}(c_i, \tau_{\mathbf{f}_j})\mathbf{b}(c_i, \mathbf{f}_j)]\} \times [\sum_{i=1}^{n} \mathbf{p}(c_i, \tau_{\mathbf{f}})\mathbf{b}(c_i, \mathbf{f})]$ (Note: $\tau_{\mathbf{f_k}}$, $1 \leq k \leq q$ refers to the time just before the application of $\mathbf{f_k}$). The total cost becomes $T[\mathbf{F}_{q+1}] = T[\mathbf{F}_q] + \Delta_T(\mathbf{f})$, where $\Delta_T(\mathbf{f}) = \mathbf{t_o}(\mathbf{f})$. Our strategy for selecting the next action is as follows: the next action $\mathbf{f}_{q+1}$ should be selected that maximizes the term $\frac{\Delta_P(\mathbf{f})}{\Delta_T(\mathbf{f})}$. Since the term $\{\prod_{j=1}^{q}[1 - \sum_{i=1}^{n} \mathbf{p}(c_i, \tau_{\mathbf{f}_j})\mathbf{b}(c_i, \mathbf{f}_j)]\}$ is fixed no matter what next action $\mathbf{f}$ is selected, our strategy becomes to select the next action that maximizes the term

$$\mathbf{E}(\mathbf{f}) = \frac{\sum_{i=1}^{n} \mathbf{p}(c_i, \tau_{\mathbf{f}})\mathbf{b}(c_i, \mathbf{f})}{\mathbf{t_o}(\mathbf{f})} \tag{8}$$

Intuitively, this approach is similar to the greedy strategy for solving KNAPSACK problem [22]. It is interesting to note that the simple greedy strategy may even generate optimal answers in certain situations (please refer to Appendix B for detail).

For the model of search agent discussed in this paper, the cost of moving the robot is much higher than the cost of changing the camera direction and visual angle size. Thus, we further simplify the "one step look ahead" problem into two separate phases: the "where to look next" phase and the "where to move next" phase. The "where to look next" task selects the parameters p, t, w, h, a for the next action to be executed when the robot position is fixed. The "where to move next" task selects the next robot position when the benefit of simply adjusting the state parameters of the camera is too low.

4 Detection Function

From Section 3 and Appendix A, we can see that the detection function $\mathbf{b}(c, \mathbf{f})$ is frequently used in calculating the probability of detecting the target and in updating the environment probability distributions. Obviously we cannot generate the value of $\mathbf{b}(c, \mathbf{f})$ at run time, so we should obtain the detection function values before the search process and retrieve these values whenever needed.

The standard detection function $\mathbf{b_0}((\theta, \delta, l), <a, w, h>)$ gives a measure of the detecting ability of the recognition algorithm a when no previous action has been applied. In this formula, $<w, h>$ is the viewing angle size of the camera; (θ, δ, l) is the relative position of the center of the target to the camera; $\theta = \arctan(\frac{x}{z})$, $\delta = \arctan(\frac{y}{z})$ and $l = z$, where (x, y, z) are the coordinates of the target center in CCS. We assume that the target is within the field of view of the camera, thus $-\frac{w}{2} \leq \theta \leq \frac{w}{2}$, $-\frac{h}{2} \leq \delta \leq \frac{h}{2}$, and $l > 0$. The value of $\mathbf{b_0}((\theta, \delta, l), <a, w, h>)$ can be obtained by experiment. We can first put the target at (θ, δ, l) and then perform experiments under various conditions, such as light intensity, background situation, and the relative orientation of the target with respect to the camera center. The final value will be the total number of successful recognitions divided by the total number of experiments. Usually, we tessellate the space of θ, δ, l into grids and record the approximate detection function value for each grid. These values can be stored in a look up table indexed by θ, δ, l and retrieved when needed. Sometimes we may approximate these values by analytic formulas.

It is not necessary to record the detection function values of all the different sizes of the solid viewing angles. We only need the detection values of one camera angle size (we call it the reference angle), and those of the other camera angle sizes can be obtained approximately by transforming them into those of the known camera angle size.

Suppose we know the detection function values for viewing angle size $<w_0, h_0>$. We want to find the detection function values for viewing angle size $<w, h>$. To get the value of $\mathbf{b}(<\theta, \delta, l>, <w, h>)$ for a given $<\theta, \delta, l>$, we need to find the values of $(\theta_0, \delta_0, l_0)$ for angle size $<w_0, h_0>$ that make the following approximation true:

$$\mathbf{b}(<\theta, \delta, l>, <w, h>) \approx \mathbf{b}(<\theta_0, \delta_0, l_0>, <w_0, h_0>) \tag{9}$$

The approximation relation (Formula 9) means that when we use the recognition algorithm to analyze the picture taken with parameters $(<\theta, \delta, l>, <w, h>)$ and the picture taken with parameters

($<\theta_0, \delta_0, l_0>$,$<w_0, h_0>$), we should get almost the same result. To guarantee this, the images of the target object should be almost the same for both imaging parameters, i.e., they must be approximately equal in at least two geometric factors, namely the scale factor and the position factor (Note, here we omit the influence of the perspective distortion). The scale factor refers to the size of the projection of the target object on the image plane. The position factor refers to the position on the image plane of the projection of the center of the target object.

We use the scale factor to find the value of l_0 when l is given. The sizes of the projection of the target object on the image planes for ($<\theta, \delta, l>$,$<w, h>$) and ($<\theta_0, \delta_0, l_0>$,$<w_0, h_0>$) are approximately determined by l and l_0, respectively. The scale factor tells us that for a target patch that is parallel to the image plane, the area of its projection on the image plane for ($<\theta, \delta, l>$,$<w, h>$) should be same as the area of its projection on the image plane for ($<\theta_0, \delta_0, l_0>$,$<w_0, h_0>$). Suppose that the width of the image plane is W and the height of the image plane is H. Since the size of the image plane remains constant for different focal lengths, W and H will be same for any focal length.

Suppose the area of the target patch is S; the area of the projected target image for ($<\theta, \delta, l>$,$<w, h>$) is S'; and the area of the projected target image for ($<\theta_0, \delta_0, l_0>$,$<w_0, h_0>$) is S'_0. From the similarity relation between the target patch and its projected image, it is easy to show that

$$S' = \frac{f^2}{l^2} S \tag{10}$$

Since

$$\tan(\frac{w}{2}) = \frac{\frac{W}{2}}{f}$$

and

$$\tan(\frac{h}{2}) = \frac{\frac{H}{2}}{f}$$

we have

$$S' = \frac{f^2}{l^2} S = \frac{WH}{4l^2 \tan(\frac{w}{2}) \tan(\frac{h}{2})} S \tag{11}$$

Similarly,

$$S'_0 = \frac{WH}{4l_0^2 \tan(\frac{w_0}{2}) \tan(\frac{h_0}{2})} S \tag{12}$$

To guarantee $S' = S'_0$, we get:

$$l_0 = l \sqrt{\frac{\tan(\frac{w}{2}) \tan(\frac{h}{2})}{\tan(\frac{w_0}{2}) \tan(\frac{h_0}{2})}} \tag{13}$$

We use the position factor to find the values of θ_0, δ_0 when θ and δ are given. Suppose D is the center of target patch with respect to ($<\theta, \delta, l>$,$<w, h>$); $D'(x', y', z')$ is the image of D on the image plane with respect to ($<\theta, \delta, l>$,$<w, h>$); D_0 is the center of target patch with respect to ($<\theta_0, \delta_0, l_0>$,$<w_0, h_0>$); and $D'_0(x'_0, y'_0, z'_0)$ is the the image of D_0 on the image plane with the

TjTT f,y,D,E,x,z,ith,eTTjTTdg,f,BTcthecennCCSenTentThnTehTTfa

Similarly,

$$y' = \frac{H}{2}\frac{\tan(\delta)}{\tan(\frac{h}{2})} \tag{15}$$

$$x'_0 = \frac{W}{2}\frac{\tan(\theta_0)}{\tan(\frac{w_0}{2})} \tag{16}$$

$$y'_0 = \frac{H}{2}\frac{\tan(\delta_0)}{\tan(\frac{h_0}{2})} \tag{17}$$

To guarantee $x' = x'_0$ and $y' = y'_0$, we get

$$\theta_0 = \arctan[\tan(\theta)\frac{\tan(\frac{w_0}{2})}{\tan(\frac{w}{2})}] \tag{18}$$

and

$$\delta_0 = \arctan[\tan(\delta)\frac{\tan(\frac{h_0}{2})}{\tan(\frac{h}{2})}] \tag{19}$$

So, when we want to find the detection function value for parameters $<\theta, \delta, l>$ with respect to the camera angle size $<w, h>$, we can first find the corresponding $<\theta_0, \delta_0, l_0>$, then retrieve the detection function value for $\mathbf{b}(<\theta_0, \delta_0, l_0>,<w_0, h_0>)$ from the look up table or from the analytical formula.

It is interesting to note that the above calculations are consistent with respect to the misfocus property of the two visual angle sizes: the area of the blur circle for $(<\theta, \delta, l>,<w, h>)$ is the same as the area of the blur circle for $(<\theta_0, \delta_0, l_0>,<w_0, h_0>)$. Suppose the diameter of the blur circle produced by $(<\theta, \delta, l>,<w, h>)$ is c, the focus distance for l is v, and the diameter of aperture is a. We have

$$\frac{c}{a} = \frac{v - f}{v} \tag{20}$$

$$\frac{1}{l} + \frac{1}{v} = \frac{1}{f} \tag{21}$$

Thus, $c = \frac{af}{l}$. Similarly, we have $c_0 = \frac{af_0}{l_0}$, where c_0 is the diameter of the blur circle produced by $(<\theta_0, \delta_0, l_0>,<w_0, h_0>)$.

Since

$$l_0 = l\sqrt{\frac{\tan(\frac{w}{2})\tan(\frac{h}{2})}{\tan(\frac{w_0}{2})\tan(\frac{h_0}{2})}} = l\frac{f_0}{f}, \tag{22}$$

we have

$$c_0 = \frac{af_0}{l_0} = \frac{af_0}{l\frac{f_0}{f}} = \frac{af}{l} = c \tag{23}$$

It is also interesting to note that when the configurations of two operations are very similar, they might be correlated with each other —– the detection function values of the second operation are influenced by the previous applied actions. For example, if we apply the same operation **f** two times, and the first application fails, then the detection function value for **f** in its second application is 0, instead of that calculated from the above described method. The reason is that the camera configurations and the surrounding environment for the two applications are same. Since this situation makes the first application of **f** fail, it will certainly make the second application of **f** fail. In order to reduce the error caused by the action correlation, we should only select those actions whose configurations are not similar. Later in this paper, we will introduce the concept of a layered sensed sphere. The actions to be selected are based on the layered sensed sphere and the configurations of these actions are quite different. Thus, the error caused by the correlation between actions can be reduced.

5 Sensed Sphere

A representation of the non-occluded space around the camera is needed. Any lines emanating from the center of the camera will hit a solid object in the environment. The environment around the camera can thus be represented by the union of all these lines. This representation can be made discrete by dividing the space around the camera with a series of solid angles. Each solid angle is associated with a radius which is the length of the line from the camera center in the direction of the central axis of the solid angle. The environment can thus be represented by the union of these solid angles. This representation is called the **sensed sphere** [51]. The sensed sphere can be constructed either by a laser or by a stereo approach. To use a stereo approach to construct the sensed sphere, we can first construct a sparse depth sampling of the environment by existing stereo algorithms [32][38][48][54] and then transform this into the representation of a sensed sphere.

In this paper, we used a laser range finder to construct the sensed sphere. In order to do this, we need to **tessellate** the surface of the unit sphere so as to get a series of uniform or near uniform patches which partition the surface. Then we can ping the laser at the center of each patch to construct the sensed sphere. There are many ways to tessellate the surface. However, in order to make the tessellation as uniform as possible and to make the number of mechanical operations as small as possible, we use the following method. First, we tessellate the range $[0, \pi]$ of tilt uniformly by a factor $2m$, where m is integer. This tessellation in general depends on the complexity of the environment. Thus, the tilt ranges are $[0, \alpha), \ldots, [(i-1)\alpha, i\alpha), \ldots, [\pi - \alpha, \pi)$, where $\alpha = \frac{\pi}{2m}$. Each tilt range $[t_{b_i}, t_{e_i})$ corresponds to a horizontal circular surface slice. The range of pan corresponding to each slice is $[0, 2\pi)$. Then, for each tilt range $[t_{b_i}, t_{e_i})$ except $[0, \alpha)$ and $[\pi - \alpha, \pi)$, we tessellate the range $[0, 2\pi)$ of pan. Each pan range $[p_{b_{i,j}}, p_{e_{i,j}})$ and its corresponding tilt range $[t_{b_i}, t_{e_i})$ defines a surface patch whose pan and tilt is confined by $t_{b_i} \leq tilt < t_{e_i}$ and $p_{b_{i,j}} \leq pan < p_{e_{i,j}}$. The goal of our tessellation is to make the areas of the resulting surface patches approximately equal.

At the equator, the change of pan is α, which is the same as the change of tilt. The area of patches at the equator is approximately α^2. However, the area of each surface patch for other *tilt*s will differ with this tessellation scheme. In order to keep patch areas approximately equal, we adjust the amount of pan for every different *tilt*. Figure 4(a) shows a surface patch on the equator and a surface patch that is not on the equator. Our strategy is to select the pan such that $| CD |=| AB |$. We then obtain that the change of pan Δ_i for tilt range $[(i-1)\alpha, i\alpha)$ is

$$\Delta_i = \begin{cases} 2\arcsin(\frac{\sin\frac{\alpha}{2}}{\sin(i\alpha)}), & \text{if } i\alpha \leq \frac{\pi}{2} \\ 2\arcsin(\frac{\sin\frac{\alpha}{2}}{\sin[(i-1)\alpha]}), & \text{if } (i-1)\alpha \geq \frac{\pi}{2} \end{cases} \tag{24}$$

So, for tilt range $[(i-1)\alpha, i\alpha)$, the pan ranges are $[0, \Delta_i), [\Delta_i, 2\Delta_i), \ldots, [n_i\Delta_i, 2\pi)$. The length of each pan range is Δ_i except for the last range $[n_i\Delta_i, 2\pi)$. When constructing the sensed sphere, we only need to change the value of pan to cover the tilt slice corresponding to tilt range $[(i-1)\alpha, i\alpha)$. After this slice is covered, we change both the values of pan and tilt to move the laser to the first position of the next tilt slice and repeat the covering process. Figure 4(b) shows a side view of a tessellation with $m = 10$. The sensed sphere constructed with the tessellation scheme described above can be concisely represented as the union of all solid angles

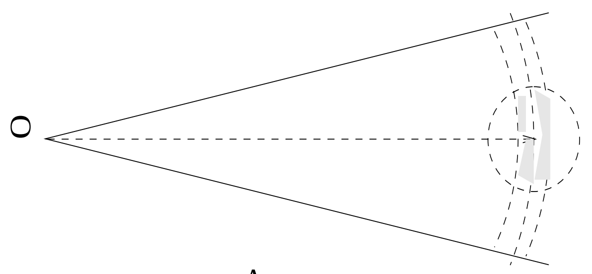

Figure 3: Solidity Property.

The illustration of the solidity property. The shaded region are assumed to be solid.

$$\bigcup_{[t_{b_i},t_{e_i})=[(i-1)\alpha,i\alpha),i=1,\ldots,2m} \left\{ \bigcup_{[p_{b_{i,j}},p_{e_{i,j}})=[0,\Delta_i),[\Delta_i,2\Delta_i),\ldots,[n_i\Delta_i,2\pi)} A_{ij}(t_{b_i},t_{e_i};p_{b_{i,j}},p_{e_{i,j}};r_{ij}) \right\}, \qquad (25)$$

where r_{ij} is the length of the radius along the direction $tilt = \frac{t_{b_i}+t_{e_i}}{2}$, $pan = \frac{p_{b_{i,j}}+p_{e_{i,j}}}{2}$. The solid angle A_{ij} is bounded by $t_{b_i} \le tilt < t_{e_i}, p_{b_{i,j}} \le pan < p_{e_{i,j}}$, and r_{ij}.

The resolution of the sensed sphere is controlled by $2m$, the number of division we use to divide $[0,\pi]$. A large value of $2m$ results in a dense sensed sphere, whereas a small value results in a crude sensed sphere. If we define the complexity of the sensed sphere to be the total number of solid angles used in the tessellation, then the complexity of the sensed sphere is less than $2m * 4m = 8m^2$. When the construction of a dense sensed sphere takes too much time, we can simply construct a crude sensed sphere during the search process.

As a by-product of sensed sphere construction, some solidity information of the environment can be obtained. When we ping the laser along a given direction, the laser will hit the environment. In real applications, we assume that a small region surrounding the point hit by laser is occupied by solid object. This information is useful when we perform the "where to move next task". In order to encode this information, each cube is associated with a solidity property. A cube is solid if we believe that it is occupied by solid object, in other words, if it is near a point hit by a laser. For each cube c, its center belongs one and only one solid angle A_c. Suppose the radius of A_c is r_{A_c} and the point hit by the laser beam along the central axis of A_c is P_{A_c}. Suppose the camera center is O. Let $\mid c - O \mid$ represent the distance between the center of c and the camera center, and $\mid c - P_{A_c} \mid$ represent the distance between c and P_{A_c}. Then for each cube c within the environment, we register its solidity property as follows. If $\mid c - O \mid \le \delta_1$ (the region within the layer in Figure 3) and $\mid c - P_{A_c} \mid \le \delta_2$ (the region within the circle in Figure 3), then the solidity of cube c is registered as *solid*, otherwise it is registered as *unknown*. Constants δ_1 and δ_2 are determined before the search process. The solid cubes can be maintained as a list during the search process. Suppose the maximum number of cubes that can be enclosed within the region determined by δ_1 and δ_2 is $N_{\delta_1\delta_2}$, then the complexity of updating the solid cube list is: $(2m) * (4m) * N_{\delta_1\delta_2}$. Usually the maximum number of solid cubes is much less than the total number of cubes n within the environment.

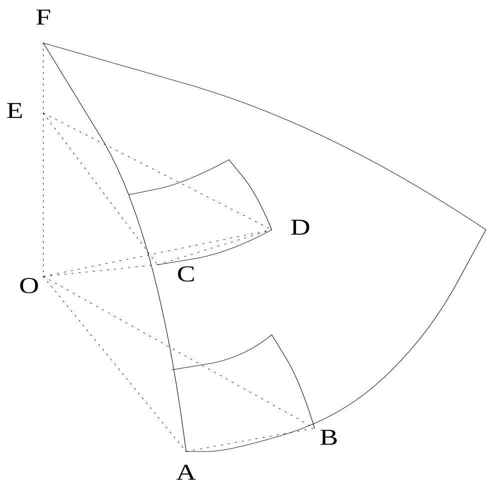

(a)

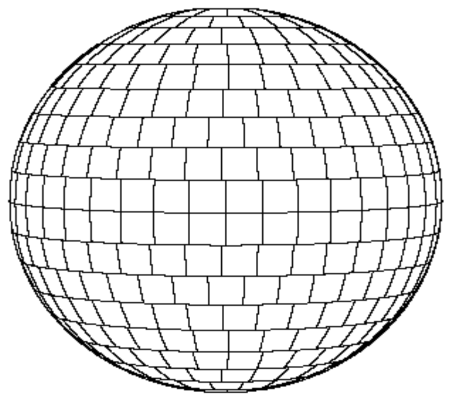

(b)

Figure 4: Tessellation of the unit sphere.

(a) The change of pan for a given tilt. (b) The side view of a tessellated sphere with $\alpha_0 = 0.157$ *(9 degrees).*

6 Where to Look Next

We need to select w, h, p, t, a such that $\mathbf{E}(\mathbf{f})$ defined in Equation 8 is maximized. We first consider the situation where only one recognition algorithm is available. Since the cost for any operation with the same recognition algorithm is the same (see assumptions in Appendix A), our task becomes the selection of w, h, p, t such that $\mathbf{P}(\mathbf{f})$ is maximized. This task is time consuming because of the huge number of possible actions, as determined by the total number of camera configurations that can be achieved by the hardware. In our case, the number of configurations is the product of: (1) the number of different viewing angle sizes; (2) the number of different pan values; and (3) the number of different tilt values. To make the problem tractable, we must decompose this huge space of possible sensing actions into a small set of actions to be tried and select the next action among the resulting limited set of actions.

6.1 Determine the Necessary Viewing Angle Size

We first select the necessary camera angle sizes. For a given robot position and a given recognition algorithm, there are many possible viewing angle sizes. However, the whole search region can be examined with high probability of detection using only a small number of them. The ability of the recognition algorithm and the value of the detection function are influenced by the image size of the target. Usually the recognizer can successfully recognize the target only when the image size of the target is within a certain range such that the whole target can be brought into the field of view of the camera and the features can be detected with the required precision. For an operation with a given recognition algorithm and a fixed viewing angle size, the probability of successfully recognizing the target is high only when the target's distance is within a certain range. Therefore, different sizes of the viewing angle $< w, h >$ will be associated with different **effective ranges** of distance. Our purpose here is to select those angles whose effective ranges will cover the entire depth D of the search region, and at the same time there will be no overlap of their effective ranges.

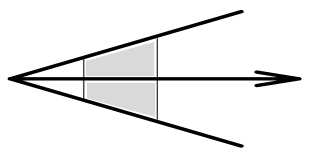
(a)

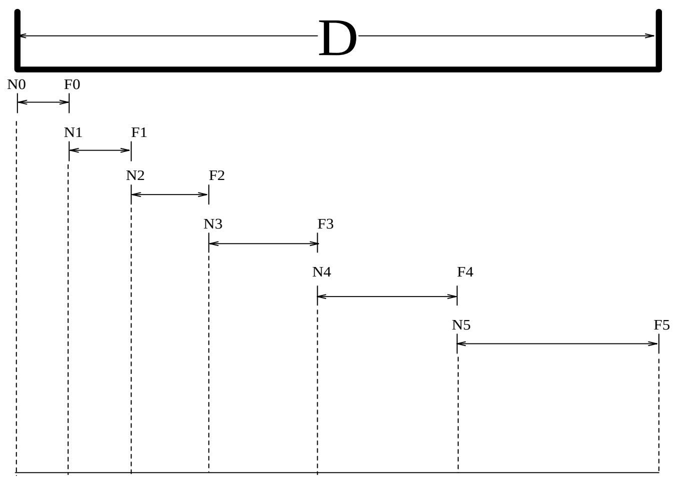

(b)

Figure 5: $2D$ illustration of the selection of the camera's angle size.

(a) The effective range of a given angle size. (b) The viewing angle size should be selected such that their effective range can cover the whole distance of the depth D and at the same time there will be no overlap of their effective ranges.

Suppose that the biggest viewing angle for the camera is $< w_0 \times h_0 >$, and its effective range is $[N_0, F_0]$. Here N refers to "Near" and F refers to "Far". We can use geometric constraint to find other required viewing angles $<w_1 \times h_1>, \ldots, < w_{n_0} \times h_{n_0}>$ and their corresponding effective ranges $[N_1, F_1], \ldots, [N_{n_0}, F_{n_0}]$, such that $[N_0, F_0] \bigcup \cdots \bigcup [N_{n_0}, F_{n_0}] \supseteq [N_0, D]$ and $[N_i, F_i) \bigcap [N_j, F_j) = \emptyset$ if $i \neq j$. These $n_0 + 1$ angle sizes are enough to examine the whole depth of the search space with high probability. Figure 5 gives a $2D$ illustration of the above idea.

Since the effective range $[N_{i+1}, F_{i+1}]$ of the next viewing angle $< w_{i+1} \times h_{i+1} >$ should be adjacent to the effective range of the current viewing angle $< w_i \times h_i >$, we have $N_{i+1} = F_i$. To guarantee that the areas of the images of the target patch of $< w_i \times h_i >$ at N_i and F_i are equal to the areas of the images of the target patch of $< w_{i+1} \times h_{i+1} >$ at N_{i+1} and F_{i+1}, respectively, we obtain (using Equations (13)):

$$w_i = 2\arctan[(\frac{N_0}{F_0})^i \tan(\frac{w_0}{2})] \tag{26}$$

$$h_i = 2\arctan[(\frac{N_0}{F_0})^i \tan(\frac{h_0}{2})] \tag{27}$$

$$N_i = F_0(\frac{F_0}{N_0})^{i-1}; F_i = F_0(\frac{F_0}{N_0})^i \tag{28}$$

Since $N_i \leq D$, we obtain $i \leq \frac{ln(\frac{D}{F_0})}{ln(\frac{F_0}{N_0})} - 1$. Let $n_0 = \lfloor \frac{ln(\frac{D}{F_0})}{ln(\frac{F_0}{N_0})} - 1 \rfloor$, then the angles to be considered by the sensing actions are $< w_0 \times h_0 >, < w_1 \times h_1 >, \ldots, < w_{n_0} \times h_{n_0} >$.

Figure 6(a) shows that for large ratio $\frac{F_0}{N_0}$, the beginning of the effective range will increase very quickly as the index of the effective camera angle increases (if the hardware can provide the corresponding angle size). Figure 6(b) shows that the total effective volume (the $3D$ space within the effective range and the viewing volume) will increase as the index of the effective camera angle

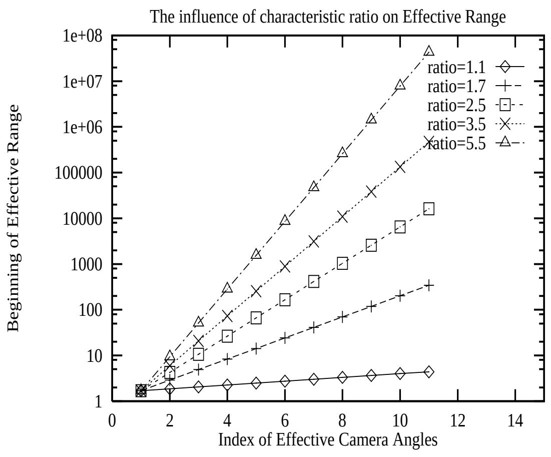

(a)

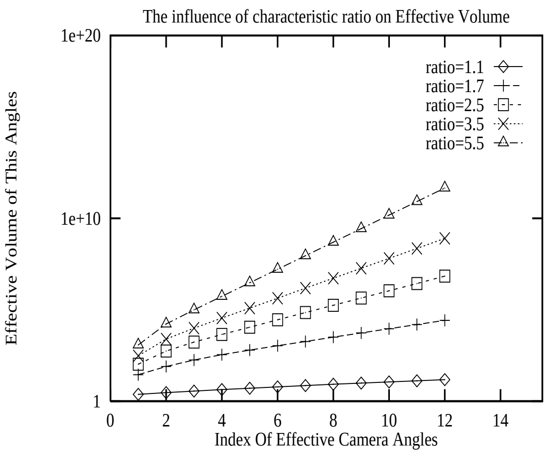

(b)

Figure 6: The Influence of the Ratio $\frac{F_0}{N_0}$.

The Influence of the Ratio $\frac{F_0}{N_0}$ *when* $N_0 = 1.7$, $w_0 = h_0 = 1.046$ *radian* (60^o)

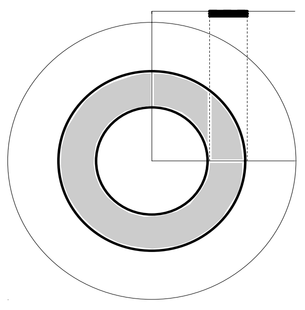

(a)

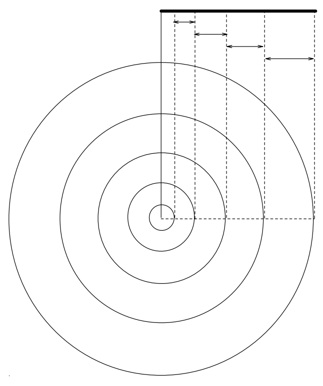

(b)

Figure 7: $2D$ illustration of the layered sensed sphere.

(a) A single layer corresponding to a given effective range. (b) The layered sensed sphere.

increases. This demonstrates that when there is no occlusion, it is better to remain in one place and search the space as far as the camera can see, rather than drive the robot near the unsearched space.

The sensed sphere can be further divided into several layers according to the effective viewing angle sizes derived above (see Figure 7 for a $2D$ illustration). This layered sensed sphere LSS can be represented as

$$LSS = \bigcup_{<w_k, h_k>, k=0,\ldots,n_0} LSS_{<w_k,h_k>}, \tag{29}$$

where $LSS_{<w_k,h_k>}$ is the layer corresponding to viewing angle size $< w_k, h_k >$,

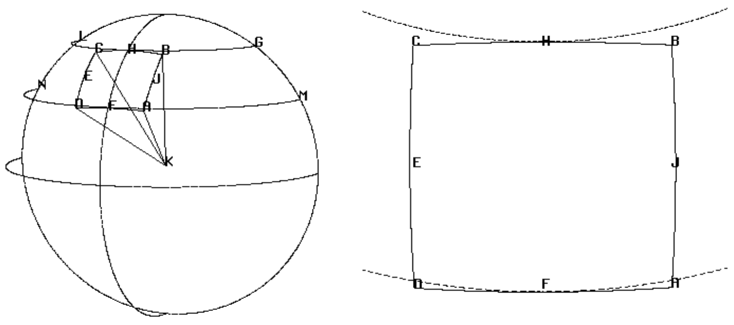

(a) (b)

Figure 8: The surface patch cut by the view volume.

(a) The camera's viewing volume and the sphere. $KABCD$ is the camera's viewing volume, where K is the center of the camera, $\widehat{AB}$, $\widehat{BC}$, $\widehat{CD}$ and $\widehat{DA}$ are the big circle arcs cut by the bounding plane of the viewing volume. $\widehat{HF}$ is the big circle arc which is cut by the vertical plane of the viewing volume (YZ plane in Camera Coordinate System). H is at the middle of big circle arc $\widehat{BC}$, F is at the middle of big circle arc $\widehat{AD}$. $\widehat{NFM}$ is part of the locus of points on the sphere whose tilt is $t + \frac{\alpha}{2}$, and $\widehat{LHG}$ is part of the locus of points on the sphere whose tilt is $t - \frac{\alpha}{2}$. $\widehat{LHG}$ and $\widehat{BC}$ only have one common point H. $\widehat{NFM}$ and $\widehat{AD}$ only have one common point F. (b) A detailed view of the surface patch $ABCD$ that is contained within the camera's viewing volume.

$$LSS_{<w_k,h_k>} = \bigcup_{i,j} LA_{ij}^{<w_k,h_k>}. \tag{30}$$

The layered solid angle slice $LA_{ij}^{<w_k,h_k>}$ is the intersection of the solid angle A_{ij} of the sensed sphere and the current layer $LSS_{<w_k,h_k>}$. There is a probability $p_{ij}^{<w_k,h_k>}$ associated with $LA_{ij}^{<w_k,h_k>}$, which gives the sum of the probabilities of all the cubes that belong to $LA_{ij}^{<w_k,h_k>}$. In other words, $p_{ij}^{<w_k,h_k>}$ is the sum of the probability for each cube which satisfies the following: (1) it is within A_{ij}; (2) the distance to the camera center is less than r_{ij}; and (3) the distance to the camera center is within the effective range of $< w_k, h_k >$, which means that the distance should be greater than $N_{<w_k,h_k>}$ and less than $F_{<w_k,h_k>}$.

6.2 Determining the Necessary Viewing Directions for a Given Angle Size

For a given effective angle size $< w, h >$ selected by the above method, there are a huge number of viewing directions that can be considered. Each direction (p, t) corresponds to a rectangular pyramid which is the viewing volume determined by parameters $< w, h, p, t >$. Within this viewing volume, only a slice of the pyramid can be examined with high detection probability by the given recognition algorithm, i.e. those parts that are within $LSS_{<w,h>}$. We call this slice of pyramid the **effective volume** for parameter $< w, h, p, t >$. The union of the effective volumes of all the possible $< p, t >$ with respect to the given $< w, h >$ will cover the given layer $LSS_{<w,h>}$. But to examine $LSS_{<w,h>}$, it is not necessary to try every possible (p, t) one by one, we only need to consider those directions such that the union of their effective volumes cover the whole layer

$LSS_{<w,h>}$ with little overlap.

The selection of the candidate directions is similar to the tessellation of the sensed sphere, but not identical. The surface patterns cut by the camera's viewing volume are different from the surface patterns obtained from our previous tessellation method. Let $\alpha = min\{w, h\}$. We study in the following how to select the necessary camera viewing directions for angle size $< \alpha, \alpha >$ such that the selected actions can cover the whole sphere.

Suppose the viewing direction of the camera (pan and tilt) is $< p, t >$. We want to determine the range of surface patch on the sphere that can be covered by the viewing volume of the camera. This covered surface patch should be specified by a tilt range $t_b \leq tilt \leq t_e$ and a pan range $p_b \leq pan \leq p_e$. Our purpose in the following is to find the values of t_b, t_e, p_b, and p_e such that the corresponding surface patch can be covered by the camera viewing volume with direction (p, t).

First, we need to find the range of pan $\Delta_{pan} = p_e - p_b$ for the given viewing direction of the camera. From Figure 8, we can see that any point J on arc $\widehat{AB}$ has a corresponding point E on arc $\widehat{CD}$ such that they have the same value of tilt. The smallest difference of pan for a point on $\widehat{AB}$ and its corresponding point on $\widehat{CD}$ occurs at point A and point D. We take the difference of the range of pan for points A and D as the value of Δ_{pan}. After a detailed calculation, we obtain

$$\Delta_{pan} = 2 \arctan\{\frac{\sin(\frac{\alpha}{2})}{\sin(t + \frac{\alpha}{2})}\}. \tag{31}$$

But for this change of pan, the viewing volume cannot cover all the surface patch whose tilt value is between $t - \frac{\alpha}{2}$ and $t + \frac{\alpha}{2}$. From Figure 8(b), we can see that the big circle arc $\widehat{HB}$ gradually goes down (decreases in Z value) as the point moves from H to B. So, there is a part between big circle arc $\widehat{CHB}$ and arc $\widehat{LHG}$ that can not be covered by the camera's viewing volume when the intended pan range is Δ_{pan}. We need to determine the tilt value of a point as it approaches B from H along the big circle arc $\widehat{HB}$ with the change of pan equal to $\frac{\Delta_{pan}}{2}$. After some calculations, we obtain the tilt value

$$\arccos\{\frac{\cos(t - \frac{\alpha}{2})}{\sqrt{1 + \frac{\sin^2(\frac{\alpha}{2})\sin^2(t - \frac{\alpha}{2})}{\sin^2(t + \frac{\alpha}{2})}}}\}.$$

From above calculations, it is easy to show that the following sphere surface patch can be covered by the viewing volume with direction (p, t),

$$p - \arctan\{\frac{\sin(\frac{\alpha}{2})}{\sin(t + \frac{\alpha}{2})}\} \leq pan \leq p + \arctan\{\frac{\sin(\frac{\alpha}{2})}{\sin(t + \frac{\alpha}{2})}\} \tag{32}$$

$$\arccos\{\frac{\cos(t - \frac{\alpha}{2})}{\sqrt{1 + \frac{\sin^2(\frac{\alpha}{2})\sin^2(t - \frac{\alpha}{2})}{\sin^2(t + \frac{\alpha}{2})}}}\} \leq tilt \leq t + \frac{\alpha}{2} \tag{33}$$

Suppose the final viewing direction set is $S_{candidate}$. According to the above calculations, we can get the following algorithm for enumerating the viewing directions to cover the whole sphere.

1. $S_{candidate} = \emptyset$

2. $p \longleftarrow 0$, $t \longleftarrow 0$, $S_{candidate} = S_{candidate} \bigcup < p, t >$.

3. $t_e \longleftarrow \frac{\pi}{2}$

4. $t_b \longleftarrow \arccos\{\frac{\cos((t_e-\frac{\alpha}{2})-\frac{\alpha}{2})}{\sqrt{1+\frac{\sin^2(\frac{\alpha}{2})\sin^2((t_e-\frac{\alpha}{2})-\frac{\alpha}{2})}{\sin^2((t_e-\frac{\alpha}{2})+\frac{\alpha}{2})}}}\}$

5. Cover the slice on the sphere whose tilt is within the range of $[t_b, t_e]$ and the slice on the sphere whose tilt is within the range of $[\pi - t_e, \pi - t_b]$.

   (a) Let $t \longleftarrow t_e - \frac{\alpha}{2}$.

   (b) let $\Delta_{pan} \longleftarrow 2\arctan\{\frac{\sin(\frac{\alpha}{2})}{\sin((t-\frac{\alpha}{2})+\frac{\alpha}{2})}\}$

   (c) Use Δ_{pan} to divide $[0, 2\pi]$ for the given slide. So, we can get a series of $[p_b, p_e]$. They are $[0, \Delta_{pan}]$, $[\Delta_{pan}, 2\Delta_{pan}]$, ..., $[k\Delta_{pan}, 2\pi]$. Note: the length of the last interval may not be Δ_{pan}.

   (d) For each division, let $p \longleftarrow \frac{p_b+p_e}{2}$. Then perform $S_{candidate} = S_{candidate} \bigcup < p, t >$ and $S_{candidate} = S_{candidate} \bigcup < p, \pi - t >$.

6. Let $t_e \longleftarrow t_b$

7. If $t_e \leq \alpha$, stop the process. Otherwise Goto 4.

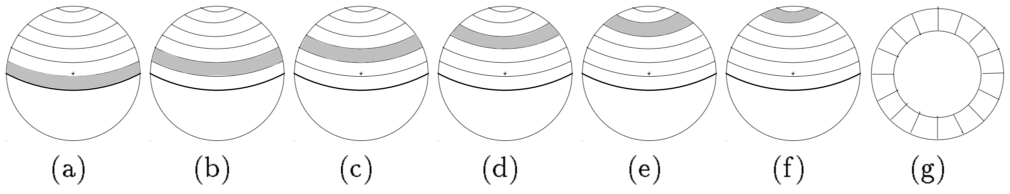

Figure 9: An example to illustrate the enumeration algorithm.

(a) We first cover the slice near the equator. The tilt interval of the slice is selected by Step 3 and Step 4. (b) After the first slice is covered, we cover the second slice. The tilt interval of the slice is selected by Step 6 and Step 4. (c), (d), (e), (f) are similar to (b). (g) An illustration on how to cover a given slice. The change of pan Δ_{pan} is determined by Step 5(b). Step 5(c) tessellate the slice using Δ_{pan}, resulting a series of blocks constrained by the tilt range and pan range as shown in (g). For each block, there is another block that is on the lower half of the sphere and is covered by Step 5(d).

6.3 Selecting the Next Action

For a given recognition algorithm a, we can find a list of candidate viewing angle sizes $w_0 \times h_0, w_1 \times h_1, \ldots, w_{n_0} \times h_{n_0}$. For each candidate angle size $< w_k, h_k >$ $(0 \leq k \leq n_0)$, we can find a series of camera viewing directions that must be considered. To select the best directions among these candidate directions, we need to use $\mathbf{P}(\mathbf{f})$ to compare them. The region that is the intersection of the sensed sphere, the corresponding layer of the given viewing angle size $< w_k, h_k >$, and the viewing volume determined by $< p, t >$ is the effective volume for $< w_k, h_k, p, t >$, denoted as $V(< w_k, h_k, p, t >)$. Since only those cubes that belong to the effective volume make major contribution to $\mathbf{P}(\mathbf{f})$, we need only take these cubes into consideration when calculating $\mathbf{P}(\mathbf{f})$. In practice, we may use the probability of the presence of the target object within the effective volume

$$\bigcup_{LA_{ij}^{<w_k,h_k>} \in V(<w_k,h_k,p,t>)} p_{ij}^{<w_k,h_k>}$$

to compare among candidate directions.

For each candidate angle size $< w_k, h_k >$ $(0 \leq k \leq n_0)$, we find a best direction $< p_k, t_k >$. Thus, we obtain $n_0 + 1$ candidate actions $\mathbf{f}_0 = \mathbf{f}(p_0, t_0, w_0, h_0, a)$, $\mathbf{f}_1 = \mathbf{f}(p_1, t_1, w_1, h_1, a)$, $\ldots$, $\mathbf{f}_{n_0} = \mathbf{f}(p_{n_0}, t_{n_0}, w_{n_0}, h_{n_0}, a)$. Then we calculate the probability of detection for each $\mathbf{f}_k$, $0 \leq k \leq n_0$ according to $\mathbf{P}(\mathbf{f})$ and select the one with highest value as the best candidate action with respect to the recognition algorithm a.

For any recognition algorithm a, we obtain a best candidate action $\mathbf{f}_{\mathbf{a}}$. Suppose a_1, a_2, $\ldots$, a_m are the recognition algorithms available for the search task, then we obtain m candidate actions $\mathbf{f}_{\mathbf{a_1}}, \ldots, \mathbf{f}_{\mathbf{a_m}}$. For each candidate action, we calculate its utility function value according to $\mathbf{E}(\mathbf{f})$. Then the action with the highest utility value will be taken as the next action to be executed.

After applying each action, we will update the probability of any cubes within the search space. Since the updating process might take time, we can select several operations under the current world state, and update the state after these operations are applied. The probability of presence within the current sensed sphere SS is $Prob_{SS} = \sum_{c_i \in SS} \mathbf{p}(c_i)$. This probability will be decreased each time an operation is applied. When the ratio of $Prob_{SS}$ and the probability of presence within the search space $\frac{Prob_{SS}}{1-\mathbf{p}(c_o)}$ is less than a certain threshold, or when the probability of detecting the target by the selected action is too small, we will want the robot to change position.

7 Where to Move Next

7.1 Selecting the Next Robot Position

The goal of the "where to move next" algorithm is to select the next camera position such that, at the new position, the camera can examine those parts of the region that have high probability of presence of the target but are occluded if viewed from the previous positions. A related, but different work is done by Maver and Bajcsy [39]. Their goal is to achieve a description of a random arrangement of unknown objects in a scene by moving the sensor to see a portion of the visual field that is hidden. Compared with randomly selecting viewing point, their approach can significantly save the computational cost by minimizing the number of views taken. For object search task, in order to select the next robot position, first we need to decide which candidate positions the camera **can reach**. Then we need to know which one is the **most beneficial** among these reachable positions. The strategy with respect to this task is greatly influenced by the hardware that controls the camera. With respect to the hardware used in this paper, the goal becomes to select the robot's next position such that the sensed sphere at the new position has the highest probability presence of the target, with the constraint that the movement of the robot from the current position to the next position is on a **straight line**.

In general, the robot can be at any position where there is no solid object within the volume occupied by the robot. Many of the possible positions are not necessary, however. If we know the geometric configuration of the search space, then we can select a set of candidate positions such that the robot can examine the whole search region without occlusion. If we have no knowledge of the geometric configuration of the search space, then we can tessellate the horizontal plane of the search region into squares and take the centers of the squares as the candidate positions to be considered. The side length of the square should be carefully designed so as to get a reasonable number of candidate positions.

The candidate positions discussed above can be further reduced by considering whether the robot can reach these positions from its current position. When the robot moves from its current position to a candidate position, there will be a volume of space that is traversed by the robot. According to the current registration of the space, if there are no solid cubes presen volume, then we assume the robot can reach this candidate position; otherwise, we assume the robot cannot reach this candidate position. We only consider those candidate positions that the robot can reach by the above criteria.

Now we will select the next robot position among these reachable candidate positions. To do this, we need to know the approximate un-occluded region that can be seen by the camera with respect to each reachable candidate position. We call this region the expected sensed sphere SS_e. If we know the geometric configuration of the search space, we can directly calculate the SS_e as shown in Figure 10(a)(b)(c). If we do not know the geometric configuration, we can estimate SS_e by using th5.000102000(c)-0ndarly bofuastheng[illegible]7000(thl)-18000(c)0(liditc)]TJ4679.99990TDΩ-0.0001TcΩ[(y)-87000.2puu
n)oas (lidn)-68999.9(ned)-69000.1(assume)-57999.9(haot)-15000(w)]TJΩ323.99990TDΩ[(e)-16000.1(iong)-5799

sphere has the maximum probability of presence of the target as our next position.

After we find the next position, we drive the robot to this position and begin our new search. Since the solidity property of the cube obtained so far may not correctly represent the real situation, the robot may stop in the middle of the journey. If it cannot reach the next position, then it will begin the "where to look next" phase at the place it has stopped.

At this point we must consider the inaccuracy of robot movement, since we need to know the robot position with respect to the world coordinate system after each movement. In general, we cannot solely depend on dead reckoning approaches, because they are not sufficiently reliable over long distances and the position error is compounded over sequences of movements as the robot traverses the environment. Here we use the method of external referencing. That is, we assume there are fixed, easily detectable landmarks or beacons in the environment. The locations of these beacons or landmarks, in the form of coordinates in the world coordinate system, serve as the reference for computing the robot position. This approach has the advantage that the position errors are bounded. Since position errors apply only to the horizontal direction (the robot height is fixed and the floor is horizontal) and are bounded, we can incorporate the associated uncertainty into the probability distribution as a blurring or convolution operation performed on the probability distribution of the cubes on each horizontal layer. For example, if we assume the robot position uncertainty is uniform and within a bounded error range, the following method can be used to incorporate this uncertainty into the probability distribution. When we move to a new place, the probability of presence of each cube will be the sum of the probabilities of presence for the cubes in the same layer within the uncertainty range centered at the corresponding cube divided by the number of these cubes. Note, this operation does not change the total sum of the probabilities of the cubes, and thus there is no need for normalization.

Please note that the "where to move next" strategy is local planning in the sense that it restricts the movement of the robot from current position to next position to be straight line. Thus, the next position selected by our strategy may not be the best position in a global sense. Please also note that our strategy implicitly assumes that the cost of adjusting the camera is much cheaper than that of moving the robot. If the two costs are comparable, then a strategy that selecting robot position and camera viewing direction and viewing angle size at the same time might perform better. For example, when the geometry structure of the environment is known, we can find a robot position such that the highest probability region can be viewed without occlusion. After the camera is directed to check this region, we then move the robot to another position such that the next highest regions can be checked without occlusion. This process can be repeated until the target is found.

7.2 The Solidity Property

During the search process, the robot must acquire information about the solidity property of the cube. This solidity property is used to calculate the radius of the expected sensed sphere. Since the movement uncertainty is bounded, the error of the calculated radius of the expected sensed sphere is also bounded. As a result, the calculated probability of presence of the expected sensed sphere with respect to each candidate position is not influenced too much by the uncertainty of the robot movement. Therefore, we ignore movement uncertainty when updating the solidity of the cubes.

After the robot drives to a new position, we use the laser to construct the sensed sphere again. After the construction, we register the space according to this new sensed sphere. We combine the new and old registration to update the registration file as shown in Table 1.

Old	New

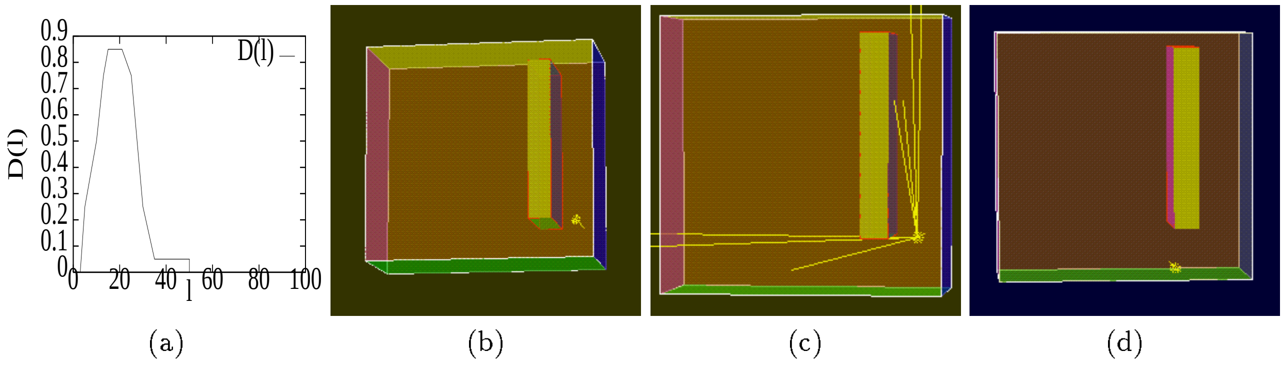

Figure 11: Simulation 1.

(a) The $D(l)$ *for detection function; (b) The environment for simulation* 1*. The size of the room is length* $\times$ *width* $\times$ *height* $= 50 \times 50 \times 25$*. There is an obstacle with size* $5 \times 37 \times 19$ *in the environment. The robot (represented by the white blob in the figure) is at position* $(45, 10)$*. The height of the robot is* 15*. (c) Top 7 actions selected at* $(45, 10)$*. The short and long lines correspond to the viewing axis of actions with angle size* $\frac{\pi}{4} \times \frac{\pi}{4}$*, and* 0.316×0.316 *respectively. (d) The next robot position* $(36, 1)$ *selected by the sensor planning system.*

within the room is uniform at the beginning. Figure 11(c) shows that the actions selected by our algorithm are used only to examine the un-occluded region. Figure 11(d) shows that the next robot position is selected to examine the region that is occluded.

The second simulation experiment is used to compare the efficiency of our strategy with the brute force strategy. The environment, the robot position and the sensor model for this simulation are the same as those of the first, except that there is no obstacle in the room. The target distribution satisfies a 3-variate normal distribution $N(\mu, \mathbf{\Sigma})$, where the mean vector $\mu = (25, 25, 15)^T$, and the covariance matrix $\mathbf{\Sigma} = diag(\sigma^2, \sigma^2, (\frac{\sigma}{2})^2)$. Three different values for σ, $\sigma = 5$, $\sigma = 15$, and $\sigma = 50$ are used in the experiment. The higher the value of σ, the higher the degree of uncertainty. The initial probability distribution is truncated to fit within the search region and is given by the following formula

$$\mathbf{p}(x, y, z) = \frac{1}{(2\pi)^{\frac{3}{2}} \times 25 \times 25 \times 15} e^{-\frac{1}{2}[\frac{(x-25)^2}{\sigma^2} + \frac{(y-25)^2}{\sigma^2} + \frac{(z-15)^2}{(\frac{\sigma}{2})^2}]} \tag{34}$$

We use $P[\mathbf{F}]$ to compare the effects of our sensor planning strategy with the effects of the Non-Planning strategy. The Non-Planning strategy means that the action application sequence is not influenced by the agent's initial knowledge of the target probability distribution. Here, the Non-Planning strategy refers to the strategy of first selecting the actions belonging to the first layer, then selecting the actions belong to the second layer, and finally, selecting the actions belong to the third layer. Figure 12 gives the effects of the two strategies for different initial probability distributions. Notice that the number of actions needed to reach the detection limit for our strategy is much smaller than that for Non-planning strategy. This illustrates that the planning strategy is more efficient.

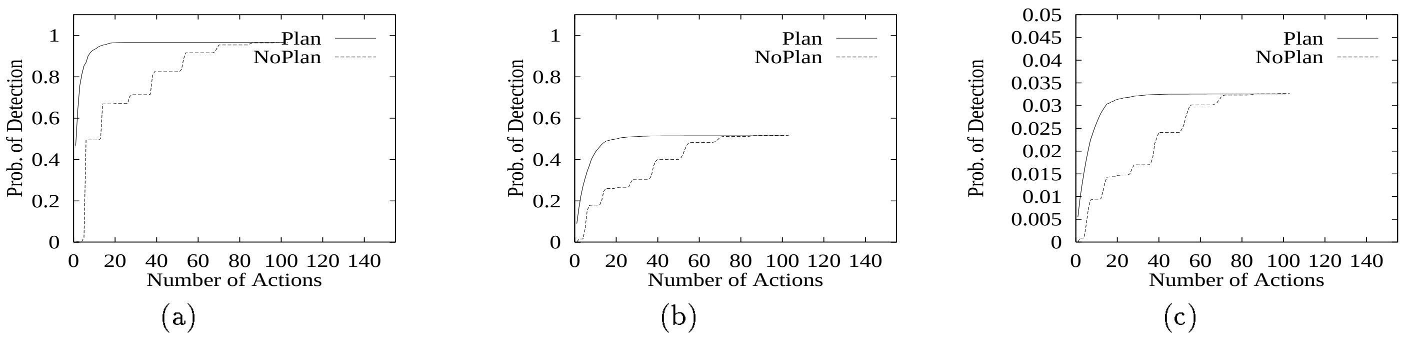

Figure 12: The detection probability.

The detection probabilities $P[\mathbf{F}]$ *of the planning strategy (Plan) and those of the Non-planning strategy (NoPlan).*
(a)$\sigma = 5$. *(b)*$\sigma = 15$. *(c)*$\sigma = 50$.

8.2 Real Environments

Real experiments are performed using the Laser Eye and the ARK robot. The search region (Figure 13) is a part of the Vision Lab of Department of Computer Science at University of Toronto. The task is to search for a white baseball within this region. This task contains three subtasks: sensor planning, hardware manipulation and object recognition. The sensor planning component is influenced by the object recognition component —– different object recognition algorithms correspond to different sensor sequences. Since our intention here is to test the sensor planning strategy rather than solving the object recognition problem, we use a simple recognition algorithm to locate the baseball within an image. Four threshold criteria are used in the recognition algorithm: intensity I_0, blob size B_{min}, B_{max}, and roundness percentage R_0. The steps of the recognition algorithm are as follows:

1. Generate a binary image from the camera's grey image using a threshold. Pixels with intensity value bigger than I_0 receive intensity value 255. Pixels with intensity value less than or equal to I_0 receive intensity value 0.
2. Perform morphological operations on the image resulting from Step 1: first erosion then dilation.
3. Perform region growing on the output image from Step 2 and label white blobs.
4. Calculate the center and size (number of pixels) of each blob.
5. According to the center and size from Step 4, calculate the corresponding circle with respect to each blob (i.e., the circle that has the same center as the blob and contains the same number of pixels as the blob), and calculate the percentage of the blob that falls into the circle.
6. If a blob size is between B_{min} and B_{max}, and more than R_0 percent of its pixels fall within the calculated circle, then this blob is taken as an image of the ball.

The first experiment uses the Laser Eye (the mobile platform is not involved) to test the "where to look next" strategy. In the experiment, the parameters for the threshold are: $I_0 = 119$,

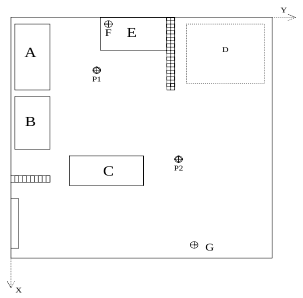

(a)

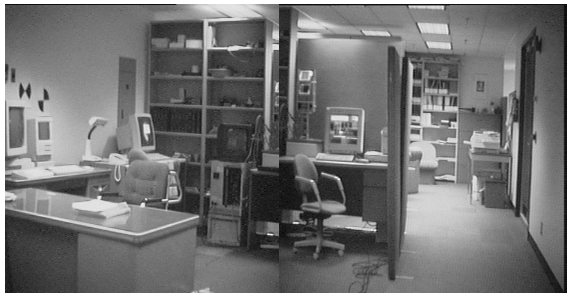

(b)

Figure 13: The search region.

(a) The configuration of the search environment (size $6m \times 5.5m \times 2.5m$). Table surfaces are labeled A, B, C, and E. The Laser Eye is at the position F of table E. D is a region on the floor. (b) Composite image of the region from position G of (a).

$B_{min} = 250$ pixels, $B_{max} = 1375$ pixels, and $R_0 = 91\%$ respectively. The Laser Eye is at F on table E (See Figure 13)(a)). We give the surface of table A, the surface of table B, and the surface of table C high target probability distribution at the beginning. The target is on table C.

First, we select the necessary angle sizes that must be used to examine the whole depth of the environment. We take the biggest angle size of the hardware $< w_0, h_0 > = < 41^o, 39^o >$ as the first angle size. The effective ranges for this angle size are obtained by experiments. The nearest distance for which the blob size is smaller than B_{max} is the value of N_0. The farthest distance for which the blob size is bigger than B_{min} is the value of F_0. We experimentally determined the effective range for $w_0 \times h_0$ as $N_0 = 1.47m$, $F_0 = 3.01m$. From equations (26), (27), and (28), we obtain the next effective angle size as $20.7^o \times 19.7^o$, and the next effective ranges are $N_1 = 3.01m$, $F_1 = 6.16m$. The output of the recognition algorithm is listed below in Table 2.

	Blob Size	Percentage		Blob Size	Percentage
N_0	1366 pixels	93.56%	N_1	1332 pixels	91.14%
F_0	273 pixels	91.58%	F_1	271 pixels	90.77%

Table 2: The output of the recognition algorithm.

From Table 2 we can see that the values of the blob size for the first angle at N_0 and F_0 are quite close to the values of the blob size for the second angle at N_1 and F_1, respectively. The process of running the recognition algorithm for angle size $< w_0, h_0 >$ at distance N_0 and angle size $< w_1, h_1 >$ at distance N_1 are shown in Figure 14.

Figure 15 shows experimental result of our search strategy. Figure 15(a) shows the sensed sphere constructed by the Laser Eye. Figure 15(b)(c)(d) are the top actions selected by our algorithm. The angle size for the first action is $41^o \times 39^o$, and the angle size for the second and third actions is $20.7^o \times 19.7^o$. Although the baseball appeared in the first image, the algorithm failed to detect it because it is outside the effective range of the action. The third action detects the target.

Note that the initial target distribution has a great influence on the performance of our sensor planning system. The reason is that the probability distribution is used to guide the sensor planning process. The more accurate is our knowledge about the initial distribution, the more efficient is our

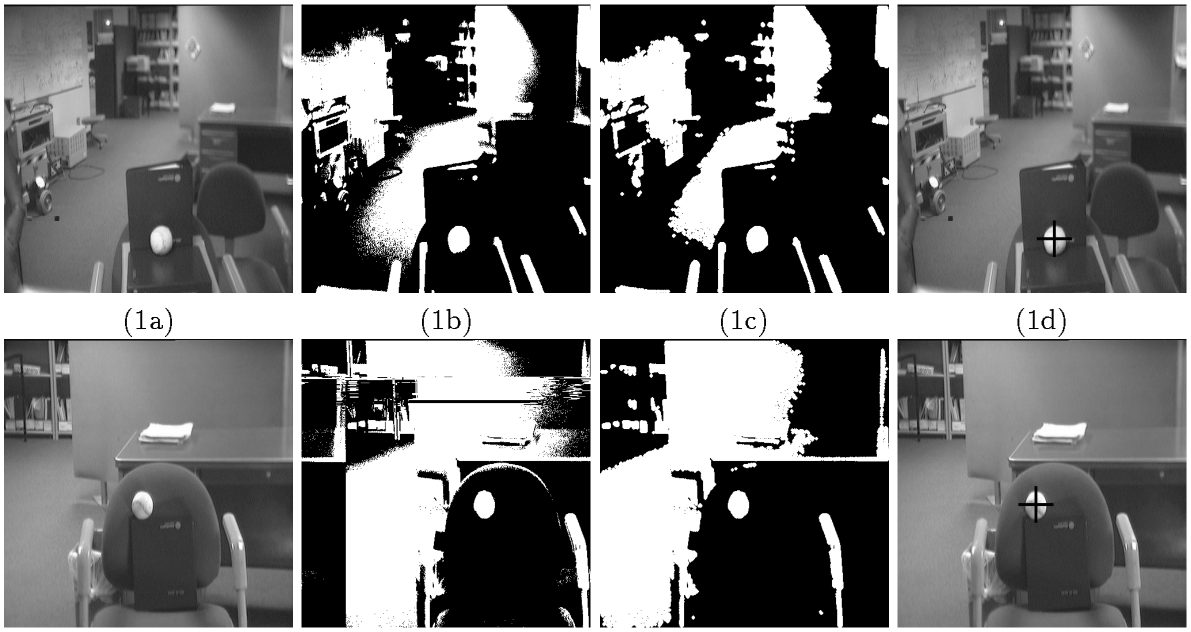
(1a) (1b) (1c) (1d)

(2a) (2b) (2c) (2d)

Figure 14: The effective range testing.

(1a) The image when angle size is $w_0 \times h_0$*. Target is 1.47m from the camera. (1b) The resultant binary image. (1c) The image after the morphological operation. (1d) The final result: target is detected. (2a) The image when angle size is* $w_1 \times h_1$*. Target is* $3.01m$ *from the camera. (2b), (2c), (2d) The recognition process applied to the image in (2a).*

algorithm. We have performed experiments to examine the influence of the initial knowledge on the effectiveness of our sensor planning strategy. Experimental results are listed in Table 3 as the average number of actions needed to bring the ball into the effective viewing volume of the camera for planning and non-planning strategies. For example, the data in the second column refers to the situation when the target is on table A. Then the number of actions needed to bring the ball into the effective volume of the camera is 1 when we give the table surface A a high probability distribution. The number of actions needed to bring the target into the effective volume of the camera by using Non-planning strategy is 8. The number of actions needed to bring the ball into the effective volume of the camera is 7 when we give the table surface C a high probability distribution (Note: the target is on A). Similar explanations can be applied to other columns of the table.

From the second and third row of Table 3, we can see that the planning strategy is much more efficient when our knowledge about the distribution is reasonable at the beginning. From the fourth row of Table 3 we can see that the performance of the planning strategy is not very satisfactory when we have the misleading information at the beginning.

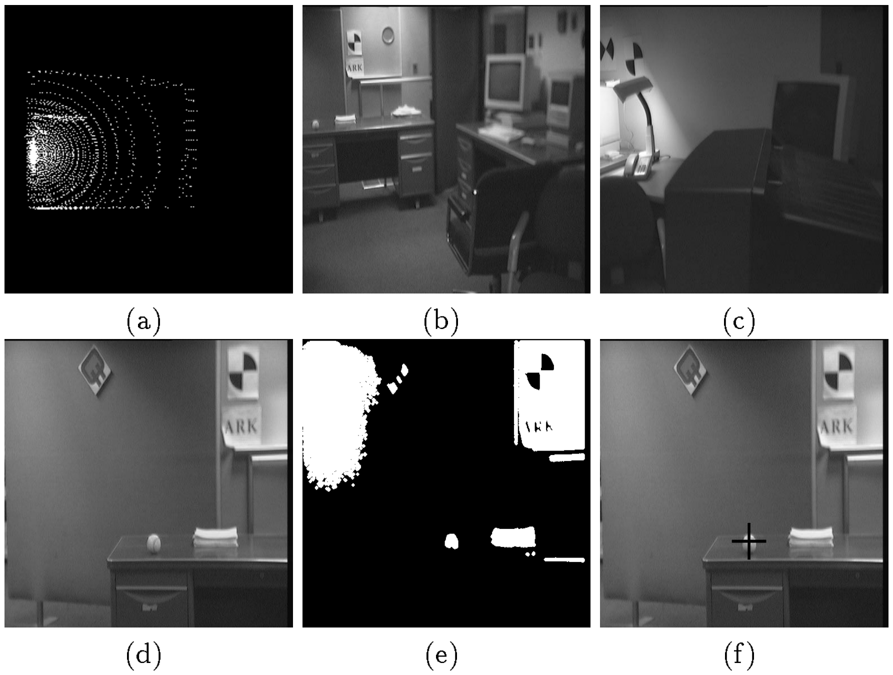

Figure 15: Where to look next experiment.

(a) Sensed sphere from Laser Eye. (b), (c), (d) The first three image sequences of the real experiment by using our planning strategy. (e) The image of (d) after region growing. (f) The result of the image analysis of (e), where the target is detected.

Target Pos.	A	B	C	A or B	A or C	A, B or C
Plan$(^{correct}_{knowledge})$	(A)1	(B)1	(C)1	(AB)1.5	(AC)1.5	(ABC)2.5
No Plan	8	9	10	8.5	9	9
Plan$(^{incorrect}_{knowledge})$	(C)7	(A)8.5	(B) 11.5	(C)6	(B)9	(C)4.3

Table 3: The comparison of planning strategy and non-planning strategy

A second experiment is used to test the whole sensor planning strategy. This time, we use the ARK robot. The configurations of the camera on the robotic head is different from that of the previous camera. The recognition algorithm is the same as that of the previous experiment, except that the threshold for the parameter values are different. Here we use $I_0 = 110$, $B_{min} = 170$ pixels, $B_{max} = 5500$ pixels, and $R_0 = 0.91$. The first viewing angle size is: $w_0 = h_0 = 30^o$. The effective range is, $N_0 = 1m$, $F_0 = 5.5m$. The outputs of the recognition algorithm are: Blob Size —– 5478 pixels for N_0 and 171 pixels for F_0; Percentage —– 92.37% for N_0 and 94.74% for F_0. Before the search process, we give the table top **B**, table top **C**, and the floor region **D** high probability of presence. The real position of the baseball is within the region **D**. When the probability of detecting the target is less then 0.0065, the robot is required to change the position.

Initially, the robot is at position $(1.6m, 2.9m)$ (P_1 of Figure 13). For this position, one angle size is sufficient. The sensed sphere constructed by the real laser at P_1 is shown in Figure 16.

Table 4 lists the actions selected by the algorithm and the corresponding detection probabilities.

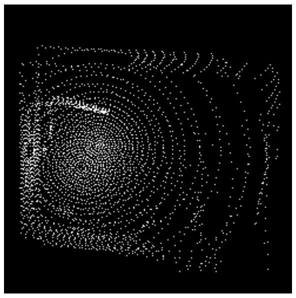

Figure 16: *The sensed sphere constructed by the robot.*

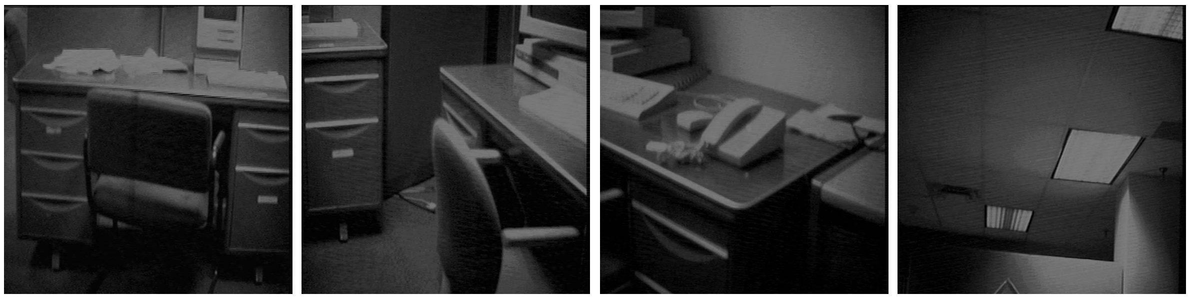

(a) (b) (c) (d)

Figure 17: Actions at the first position.

The four actions generated by the sensor planning algorithm. Images are shown for (a) tilt = 1.801100 *and pan* = 0.000000. *(b) tilt* = 2.315700, *pan* = 5.655361. *(c) tilt* = 2.315700, *pan* = 4.948441. *(d) tilt* = 1.286500, *pan* = 5.366405.

Tilt	**Pan**	**Probability of Detection**
1.801100	0.000000	0.037403
2.315700	5.655361	0.036140
2.315700	4.948441	0.036654
1.286500	5.366405	0.006105

Table 4: The actions selected by the algorithm and the corresponding detection probabilities.

Figure 17 shows the four images taken by the head according to the four actions listed above. We can see that the first action examines table **C**, the second and third actions examine table **B**. The fourth action simply points upward, and none of the specified regions is examined. The probability of detecting the target by the fourth action is very low, because none of the high probability regions is brought into the effective volume of the camera. No action is selected to check region **D**, because **D** is occluded by the office wall.

Since the probability of detection of the last action is 0.006105, which is less than 0.0065, the robot will quit the "where to look next" process and begin the "where to move next" process. The candidate positions are those for which $x = 0.1m$, $0.6m$, $1.1m$, ..., $6.1m$ and $y = 0.1m$, $0.6m$, $1.1m$, ..., $5.6m$. Figure 18 (a) shows the probability of the expected sensed sphere for each reachable candidate position. Among them, the position $(4.6m, 3.6m)$ (P_2 in Figure 13(b) has the maximum probability. Figure 18 (b) shows the expected sensed sphere for position $(4.6m, 3.6m)$, where the white points represent the calculated intersecting points of the emanating lines from the

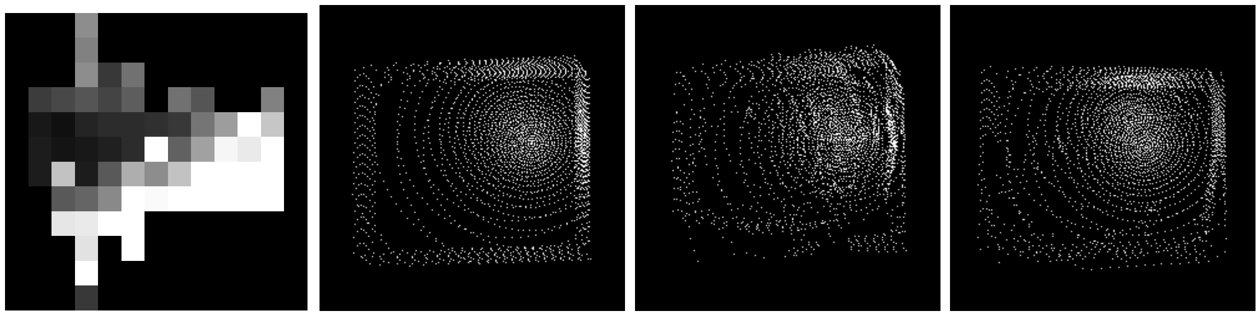
(a) (b) (c) (d)

Figure 18: Where to move next.

(a) The probability of presence for each reachable candidate position, the brighter the pixel intensity, the higher the probability. (b) The expected sensed sphere at position $(4.6m, 3.6m)$ *by only considering the boundary of the search region. (c) The expected sensed sphere after constraining using the solid cubes. (d) The real sensed sphere constructed at the position* $(4.6m, 3.6m)$.

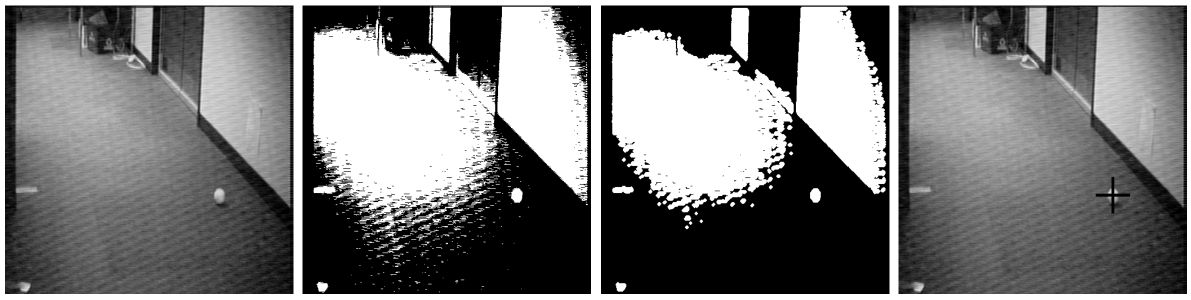
(a) (b) (c) (d)

Figure 19: Actions at the second position.

(a) The image of the first action. (b) The generated binary image. (c) The image after the morphological operation. (d) The final result: the target is detected (blob size is 372*, percentage is* 91.40%*).*

camera center and the boundary of the search region. Figure 18(c) shows the sensed sphere when constrained by the solid cubes at this position, where the white points represent the calculated intersecting points of the emanating lines from the camera center and the environment after updating the radius using solid cubes. When the robot drives to the next position $(4.6m, 3.6m)$, it constructs the sensed sphere and repeats the search process. Figure 18(d) shows the sensed sphere constructed by the robot, where the white points represent the intersections of the real environment and the laser beams emanating from the camera center.

At the new position, the robot begins the search process again. The first action is: $tilt = 2.315700$ (radian) and $pan = 3.534601$ (radian). This action find the target. Figure 19 shows the image of this action and the image processing results.

It is interesting to note that the performance of the object recognition algorithm has a great influence on the sensing strategy of the search agent. Suppose we have applied an action and failed to detect the target. If the recognition algorithm has high detection ability, then the probabilities of those cubes within the effective volume will drop greatly as a result of probability updating. Thus, there is less tendency that the corresponding region will be examined again from other viewpoint. If the recognition algorithm has low detection ability, then the probability updating will have less influence on the probabilities within the effective volume, and this region will have more chance to be examined again from other viewpoint.

9 Conclusion

An interesting phenomenon of most past computer vision research is that the purely theoretical side of computer vision is heavily emphasized. Consequently, many theoretical results cannot be applied to real situations, because they are obtained by making unrealistic assumptions. We think it is beneficial to put more emphasis on the "task oriented vision" framework as an alternative to the classic reconstructionist paradigm. For this new framework, the vision system is just one component of the agent embedded in the world, and it should provide only the minimum perceptual functionality the agent needs to perform whatever it is doing at the moment.

Object search is a typical task for this new framework. For this task, the vision module involved is object recognition. In order to find the target, the agent has to purposefully change the sensing parameters so as to bring the target into the field of view of the camera and to make the image of the target easily recognized by the available recognition algorithms. The study of the object search task may generate insight into existing vision problems. For example, the problem of object recognition may be less difficult when the image is intelligently grabbed by a controlled camera and the image analysis is interpreted within specific contexts. Research shows that the object recognition problem can be simpler if the camera is intelligently controlled [58]. Of course, the simplicity obtained in the image analysis phase is at the cost of the complexity encountered in the camera controlling phase. Much work has been done on image analysis. It is now time to study the problems related to the control of the camera. This is one reason why the sensor planning task for object search should be studied and comprises one of the motivations of this paper.

In this paper, we study the problem of sensor planning for object search from both the aspect of theory and that of practical implementation. By introducing the concept of a detection function for the object recognition algorithm and the concept of a probability distribution for the target within the search region, we formulate the sensor planning task as an optimization problem: the goal is to maximize the probability of detecting the target within a given time constraint. By analyzing the formulation of the problem, we obtain some important properties of this task and find that this task is NP-complete in general. In order to make the problem tractable, we propose to use the greedy strategy, and point out that under some special conditions this strategy may generate an optimal answer. By considering the detection ability of operations, we are able to decompose the enormous space of possible sensing actions into a limited finite set of actions that must be tried, thus greatly reducing the complexity in the action selection process. Various simulation experiments and real experiments have been performed based on our strategy. Experimental results show that our strategy is more efficient than those strategies with fixed action sequences (non-planning). It is interesting to note here that Wixson [60] has examined the "where to move next" problem in $2D$ situations by simulation and concluded that simpler model-free methods can find objects without significantly more effort than a map-based method. His result does not contradict our result because the probability distribution is not considered in his experiments.

Our theory has been applied using the ARK robot and the Laser Eye. Experiments so far have been successful as a proof of concept. A future direction is the design of a search strategy when the target is able to move. In this case, the probability updating process will be much more complex.

Because we have to consider not only the influence of actions on the probabilities of the region, but also the influence of the movement of the target on the probabilities of the region. Another direction of research is the design of a search strategy when several robots are available.

A The Complexity of the Sensor Planning Task

Complexity level analysis of robotics and vision problems is important because it can reveal basic insights into the structure of the problem and delimit the space of permissible solutions in a formal and theoretical fashion. In this section, we first pinpoint some important properties of the task and then outline the proof that the sensor planning task is NP-complete.

From the definition of the sensor planning task, we can see that the probability of detecting the target by an effort allocation is represented by a complex formula with many intermediate probability distributions $\mathbf{p}(c,\tau)$. Since this distribution is updated every time an action is applied, it is hard to see any regularities in the expression $P[\mathbf{F}]$ defined above. Suppose $\mathbf{p}(c_1,\tau_0), \mathbf{p}(c_2,\tau_0), \ldots, \mathbf{p}(c_n,\tau_0), \mathbf{p}(c_o,\tau_0)$ represent the initial probability distribution, $P(\mathbf{f}_i,\tau_0) = \sum_{j=1}^{n} \mathbf{p}(c_j,\tau_0)\mathbf{b}(c_j,\mathbf{f}_i)$ represents the probability of detecting the target by applying the action $\mathbf{f}_i$ when no action has been applied before.

If we can obtain a general expression of the target distribution at any time during the search process, then we are able to figure out how the distribution changes as a result of action applications. This might simplify the computations of the probability updating process. In Lemma 1, we give such an expression.

Lemma 1 *Suppose $\langle \mathbf{f}_1,\ldots,\mathbf{f}_k\rangle$ are the ordered actions applied during the search process, then the resulting target probability distribution is given by:*

$$\mathbf{p}(c,\tau_k) = \mathbf{p}(c,\tau_0)\frac{[1-\mathbf{b}(c,\mathbf{f}_1)][1-\mathbf{b}(c,\mathbf{f}_2)]\ldots[1-\mathbf{b}(c,\mathbf{f}_k)]}{[1-P(\mathbf{f}_1)][1-P(\mathbf{f}_2)]\ldots[1-P(\mathbf{f}_k)]}, \tag{35}$$

where $\mathbf{p}(c,\tau_k)$ gives the probability for cube c after actions $\langle \mathbf{f}_1,\ldots,\mathbf{f}_k\rangle$ are applied.

When $k = 1$, the above gives the calculation needed to update the target distribution after an action is applied. The cost to calculate $P(\mathbf{f}_k)$ is at most n, because we only need to consider those cubes that is within the field of view of $\mathbf{f}$. The updating process for all the cubes within the environment takes $n+1$ computations. Thus at most $2n$ operations are needed to update the environment.

For a given robot position, the probability updating process can be further simplified by only updating the probabilities of those cubes that is within the current sensed sphere. The probability updating process for cubes outside current sensed sphere can be postponed until the robot has finished searching at the current position. The following gives the reason. For cubes outside the current sensed sphere, since its detection function value is 0, we can get the updating rule as following:

$$\mathbf{p}(c,\tau_k) = \frac{\mathbf{p}(c,\tau_0)}{[1-P(\mathbf{f}_1)][1-P(\mathbf{f}_2)]\ldots[1-P(\mathbf{f}_k)]} \tag{36}$$

Thus, we only need to keep a record of $P(\mathbf{f}_i)$ for each unsuccessful action $\mathbf{f}_i$. When the robot decides to move to another position, we then update the probabilities for those cubes that is outside the current sensed sphere according to Formula 36.

If we can represent $P[\mathbf{F}]$ just by the initial probability distributions, we might gain some insight and deeper understanding of the properties of $P[\mathbf{F}]$. The following lemma illustrates this idea.

Lemma 2 *For a given allocation $\mathbf{F} = \{\mathbf{f}_1, \ldots, \mathbf{f}_q\}$, we have*

$$\begin{aligned}
P[\mathbf{F}] &= \sum_{i_1=1}^{q} P(\mathbf{f}_i, \tau_0) \\
&\quad +(-1)^{2+1} \sum_{1 \le i_1 < i_2 \le q} \Big(\sum_{c \in \Omega(\mathbf{f}_{i_1}) \bigcap \Omega(\mathbf{f}_{i_2})} \mathbf{p}(c,\tau_0)\mathbf{b}(c,\mathbf{f}_{i_1})\mathbf{b}(c,\mathbf{f}_{i_2}) \Big) \\
&\quad + \ldots \\
&\quad +(-1)^{r+1} \sum_{1 \le i_1 < i_2 < \ldots < i_r \le q} \Big(\sum_{c \in \Omega(\mathbf{f}_{i_1}) \bigcap \Omega(\mathbf{f}_{i_2}) \bigcap \ldots \bigcap \Omega(\mathbf{f}_{i_r})} \mathbf{p}(c,\tau_0)\mathbf{b}(c,\mathbf{f}_{i_1})\mathbf{b}(c,\mathbf{f}_{i_2}) \ldots \mathbf{b}(c,\mathbf{f}_{i_r}) \Big) \\
&\quad + \ldots \\
&\quad +(-1)^{q+1} \Big(\sum_{c \in \Omega(\mathbf{f}_1) \bigcap \Omega(\mathbf{f}_2) \bigcap \ldots \bigcap \Omega(\mathbf{f}_q)} \mathbf{p}(c,\tau_0)\mathbf{b}(c,\mathbf{f}_1) \ldots \mathbf{b}(c,\mathbf{f}_q) \Big) \qquad (37)
\end{aligned}$$

where $\Omega(\mathbf{f}) = \{c \mid \mathbf{b}(c,\mathbf{f}) \neq 0\}$ is called the influence range of action $\mathbf{f}$, which gives the region such that the detection function value of $\mathbf{f}$ is not zero (that is, it is possible for $\mathbf{f}$ to detect the target if the target center is within the region). See [64] [61] for proofs.

From Lemma 2 it is easy to see that $P[\mathbf{F}]$ is not influenced by the order of the applied actions. This result agrees with common knowledge, because for a given set of actions, the expected probability of detecting the target should be the same regardless of the order of applications. For example, if we have 3 actions $\mathbf{f}_1$, $\mathbf{f}_2$, $\mathbf{f}_3$ and the following are two orders of their application: (A) $\mathbf{f}_1 \to \mathbf{f}_2 \to \mathbf{f}_3$; (B) $\mathbf{f}_3 \to \mathbf{f}_1 \to \mathbf{f}_2$. Suppose sequence (A) detects the target, then at least one of them detects the target. Not losing generality, let it be $\mathbf{f}_1$. Suppose $\mathbf{f}_1 = \mathbf{f}(x_c, y_c, z_c, p, t, w, h, a)$. Then the event $\mathbf{f}_1$ of (A) detects the target implys that when the camera position is (x_c, y_c, z_c), the camera viewing direction is p, t, the camera angle size is w, h, and the recognition algorithm is a, the target will be detected. This definitely implys that $\mathbf{f}_1$ of (B) also detects the target. Which means that sequence (B) detects the target. Similarly, if sequence (A) can not detect the target, so cannot sequence (B). Thus, sequence (A) and sequence (B) have the same chance of detecting the target. Therefore, the expected probability of detecting the target is same regardless of the order of applications.

As a direct result of Lemma 2, we have the following lemma which can be used to prove that the sensor planning task is NP-complete.

Lemma 3 *For an allocation $\mathbf{F} = \{\mathbf{f}_1, \ldots, \mathbf{f}_q\}$, if we restrict the available actions such that no cube belongs to any two influence ranges, i.e., $\Omega(\mathbf{f}_i) \bigcap \Omega(\mathbf{f}_j) = \emptyset$ for $i \neq j$, then $P[\mathbf{F}]$ can be calculated by the following:*

$$P[\mathbf{F}] = \sum_{i=1}^{q} P(\mathbf{f}_i, \tau_0) \qquad (38)$$

To prove that the sensor planning task for object search is *NP-complete*, we first change the maximization problem into the equivalent decision problem. It is obvious that the resulting problem belongs to NP. After restricting the resulting problem by only allowing instances in which any two available operations do not have common influence range, we are able to prove that the restricted problem is equivalent to the *KNAPSACK* problem. Thus sensor planning for object search task is NP-complete. Please refer to [64] [61] for detail.

B Properties of the Greedy Strategy

In some situations, the simple greedy strategy may even generate optimal answers. By using Lemma 3, we can prove the following result.

Lemma 4: *Suppose the available operations* $\mathbf{O}_\Omega = \{\mathbf{f}_1, \mathbf{f}_2, \ldots, \mathbf{f}_q\}$ *satisfy:*
(1) $\mathbf{t_o}(\mathbf{f}_i) = \mathbf{t_o}(\mathbf{f}_j)$, $1 \le i, j \le q$.
(2) $\Omega(\mathbf{f}_j) \bigcap \Omega(\mathbf{f}_i) = \emptyset$, $1 \le i, j \le q, i \ne j$.
Then, the above greedy strategy generates optimal answer.

It is interesting to note that the greedy strategy can sometimes minimize the expected time to detect the target. For a given effort allocation $\mathbf{F} = \{\mathbf{f}_1, \ldots, \mathbf{f}_k\}$, the expected time to detect the target by applying $\mathbf{F}$ is defined as

$$\begin{aligned} \Theta[\mathbf{F}] \;=\; & \mathbf{t}(\mathbf{f}_1) \times P(\mathbf{f}_1) \\ & + \Big(\mathbf{t}(\mathbf{f}_1) + \mathbf{t}(\mathbf{f}_2)\Big) \times [1 - P(\mathbf{f}_1)]P(\mathbf{f}_2) \\ & + \ldots \\ & + \Big(\mathbf{t}(\mathbf{f}_1) + \ldots + \mathbf{t}(\mathbf{f}_k)\Big) \times \{\prod_{i=1}^{k-1}[1 - P(\mathbf{f}_i)]\}P(\mathbf{f}_k) \end{aligned} \tag{39}$$

For $\Theta[\mathbf{F}]$ defined above, we have the following result.

Property 1 *For a group of actions* $\{\mathbf{f}_1, \ldots, \mathbf{f}_q\}$, *if there is no cube belonging to any two action ranges:* $\Omega(\mathbf{f}_j) \bigcap \Omega(\mathbf{f}_i) = \emptyset$, *if* $i \ne j$, *then the application order of the actions selected by our strategy minimizes the expected time of detecting the target with respect to this group.*

Please refer to [61] for proofs.

References

[1] A. Abbott and N. Ahuja. Surface reconstruction by dynamic integration of focus, camera vergence, and stereo. In *Second International Conference on Computer Vision*, pages 532–543, Florida, USA, December 1988.

[2] A.L.Abbott. Selective fixation control for machine vision: A survey. In *IEEE Intervnational Conference on System, Man and Cybernetics*, pages 1–6, August 1991.

[3] Y. Aloimonous, I. Weiss, and A. Bandyopadhyay. Active vision. In *First International Conference on Computer Vision*, pages 35–54, London, England, June 1987.

[4] R. Bajcsy. Active perception vs. passive perception. In *Third IEEE Workshop on Vision*, pages 55–59, Bellaire, 1985.

[5] R. Bajcsy and M. Campos. Active and exploratory perception. *CVGIP: Image Understanding*, 56(1):31–40, 1992.

[6] A. Balke and A. Yuille. *Active Vision.* The MIT Press, Cambridge, Mass., 1992.

[7] D. Ballard. Animate vision. *Artificial Intelligence*, 48:57–86, 1991.

[8] D. H. Ballard. Task frames in visuo-motor coordination. In *Proceedings IEEE Workshop on Computer Vision: Representation and Control*, pages 3–10, Bellaire MI., 1985.

[9] D. H. Ballard and A. Ozcandarli. Eye fixation and early vision: Kinetic depth. In *Second International Conference on Computer Vision*, pages 524–531, Florida, USA, December 1988.

[10] R. Bolle, A. Califano, and R. Kjeldsen. Data and model driven foveation. Technical Report RC 15096, IBM Research Division, T.J. Watson Research Center, NY, October 1989.

[11] M. Brand. An eye for design: Why, where and how to look for causal structure in visual scenes. *SPIE.Intelligent Robots and Computer Vision*, 1825(XI):180–188, 1992.

[12] R. Brooks. Intelligence without representation. *Artificial Intelligence*, (47):139–160, 1991.

[13] C. Brown. Issues in selective perception. In *11th International Conference on Pattern Recognition*, pages 21–30, 1992.

[14] Connel. *An Artificial Creature.* PhD thesis, AI Lab, MIT, 1989.

[15] C. K. Cowan and P. D. Kovesi. Automatic sensor placement from vision task requirements. *IEEE Transactions on Pattern analysis and Machine Intelligence*, 10(3):407–416, May 1988.

[16] S. Culhane and J. Tsotsos. An attentional prototype for early vision. In *Second European Conference on Computer Vision*, pages 551–560, Santa Margherita Ligure, Italy, May 1992.

[17] T. Dean. Sequential decision making for active perception. In *Image Understanding Workshop*, pages 889–894, Pennsylvania, USA, September 1990.

[18] S. Dickinson, H. Christensen, J. Tsotsos, and G. Olofsson. Active object recognition integrating attention and viewpoint control. *Computer Vision and Image Understanding*, 67(3):239–260, September 1997.

[19] T. D. Garvey. Perceptual strategies for purposive vision. Technical Report Technical Note 117, SRI International, 1976.

[20] J. Gibson. *The perception of the visual world.* Houghton-Mifflin, Boston, 1950.

[21] J. Gibson. *The Ecological Approach to Visual Perception.* Houghton-Mifflin, Boston, 1979.

[22] E. Horowitz and S. Sahni. *Fundamentals of Computer Algorithms.* Pitman Publishing Limited, 39 Parker Street, London WC2B 5PB, 1978.

[23] D. Hubel. *Eye, Brain and Vision.* Volume 22 of Scientific American Library W.H.Freeman and Company, 1988.

[24] S. Hutchinson and A. Kak. Spar: A planner that satisfies operational and geometric goals in uncertain environments. *AI Magazine*, 11(1):30–61, 1990.

[25] P. Jasiobedzki, M. Jenkin, E. Milios, B. Down, and J. Tsotsos. Laser eye - a new 3d sensor for active vision. In *Intelligent Robotics and Computer Vision: Sensor Fusion VI. Proceedings of SPIE. vol. 2059*, pages 316–321, Boston, Sept. 1993.

[26] F. Jensen, H. Christensen, and J. Nielsen. Baysian methods for interpretation and control in multiagent vision systems. In *K. Bowyer, editor, SPIE Applications of AI X: Machine Vision and Robotics, volume 1708*, pages 536–548, Orlando, FL, April 1992.

[27] T. K., P. Allen, and R. Tsai. A survey of sensor planning in computer vision. Technical report, Comp. Sci. Dept., Columbia University, 1992.

[28] J. Kender and Freudenstein. What is a “degenerate” view? In *Image Understanding Workshop*, pages 589–598, California, February 1987.

[29] H. Kim, R. Jain, and R. A. Volz. Object recognition using multiple views. In *1985 IEEE Intervnational Conference on Robotics and Automation*, pages 28–33, July 1985.

[30] J. Koenderink and A. van Doorn. The internal representation of solid shape with respect to vision. *Biological Cybernetics*, 32:211–216, 1979.

[31] B. O. Koopman. *Search and Screen: general principles with historical applications.* Pergaman Press, Elmsford, N.Y, 1980.

[32] D. J. Kriegman, E. Triendl, and T. O. Binford. Stereo vision and navigation in building for mobile robots. *IEEE Transactions on Robotics and Automation*, 5(6):792–803, December 1989.

[33] E. Krotkov. Focusing. *International Journal of Computer Vision*, 1:223–237, 1987.

[34] E. Krotkov. *Active computer vision by cooperative focus and stereo.* Springer-Verlag, New York, 1989.

[35] K. Kutulakos and Dyer. Recovering shape by purposive viewpoint adjustment. In *Proceedings of Computer Vision and Pattern Recognition*, pages 16–22, Illinois,USA, June 1992.

[36] T. Levitt, J. Agosta, and T. Binford. Baysian methods for interpretation and control in multiagent vision systems. In *K. Bowyer, editor, SPIE Applications of AI X: Machine Vision and Robotics, volume 1708*, pages 536–548, Orlando, FL, April 1992.

[37] S. Li. Realizing active vision by a mobile robot. In *IEEE Workshop on Visual Motion*, pages 205–209, 1991.

[38] L. Mathies and S. A. Shafer. Error modeling in stereo navigation. *IEEE Journal of Robotics and Automation*, RA-3(3):239–248, 1987.

[39] J. Maver and R. Bajcsy. How to decide from the first view where to look next. In *Proceedings of the DARPA Image Understanding Workshop*, September 1990.

[40] J. Maver and R. Bajcsy. Occlusions and the next view planning. In *IEEE 1992 International Conference on Robotics and Automation*, pages 1806–1811, April 1992.

[41] R. C. Nelson. Imtroduction: Vision as intelligent behavior: An introduction to machine vision at the university of rochester. *International Journal Computer Vision*, 7(1), 1991.

[42] S. Nickerson, M. Jenkin, E. Milios, B. Down, P. Jasiobedzki, A. Jepson, D. Terzopoulos, J. Tsotsos, D. Wilkes, N. Bains, and K. Tran. Ark: Autonomous navigation of a mobile robot in a known environment. In *Intelligent Autonomous Systems-3*, pages 288–296, Pennsylvania, USA, February 1993.

[43] R.A.Brooks and J.H.Connell. Asynchronous distributed control system for a mobile robot. In *Mobile Robots:Proc. SPIE 727*, California, 1987.

[44] R. Rimey and C. Brown. Where to look next using a bayes net: Incorporating geometric relations. In *Second European Conference on Computer Vision*, pages 542–550, Santa Margherita Ligure, Italy, May 1992.

[45] A. Shmuel and Werman. Active vision:3d from an image sequence. In *10th International Conference on Pattern Recognition*, pages 48–54, New Jersey, USA, June 1990.

[46] M. Swain and M. Stricker. Promising directions in active vision. Technical Report CS 91-27, Univ. Of Chicago Technical Report, 1991.

[47] K. Tarabanis, R. Y. Tsai, and P. K. Allen. Analytical characterization of the feature detectability constraints of resolution, focus, and field of view for vision sensor planning. *CVGIP: Image Understanding*, (59):340–358, May 1994.

[48] C. E. Thorpe, M. Hebert, T. Kanade, and S. Shafer. Vision and navigation for the carnegie-mellon navlab. *IEEE Transactions on Pattern Analysis and Machine Intelligence*, 10(3):362–373, May 1988.

[49] J. Tsotsos. A complexity level analysis of immediate vision. *International Journal Computer Vision*, 4(1):303–320, 1988.

[50] J. Tsotsos. Analyzing vision at the complexity level. *The behavioral and brain science*, 13:423–469, 1990.

[51] J. Tsotsos. 3d search strategy. *Internal ARK Working Paper, Department of Computer Science, Univrsity of Toronto*, 1992.

[52] J. Tsotsos. Active verses passive perception, which is more efficient? *IJCV*, 1992.

[53] J. Tsotsos. On the relative complexity of active vs. passive visual search. *International Journal of Computer Vision*, 7:127–141, 1992.

[54] M. A. Turk, D. G. Morgenthaler, K. D. Gremban, and M. Marra. Vits —– a vision system for autonomous land vehicle navigation. *IEEE Transactions on Pattern Analysis and Machine Intelligence*, 10(3):362–373, May 1988.

[55] W.E.Grimson. Sensing strategies for disambiguating among multiple objects in known poses. *IEEE Journal of Robotics and Automation*, RA-2(4):196–213, December 1986.

[56] P. Whaite and F. P. Ferrie. From uncertainty to visual exploratory. *IEEE Transactions on Pattern Analysis and Machine Intelligence*, 13(10):1308–1049, 1991.

[57] D. Wilkes. Active object recognition. Technical report, Department of Computer Science, University of Toronto, 1994.

[58] D. Wilkes and J. Tsotsos. Active object recognition. In *Proceedings of Computer Vision and Pattern Recognition*, pages 136–141, Illinois, USA, June 1992.

[59] L. Wixson and D. Ballard. Using intermediate object to improve the efficiency of visual search. *International Journal on Computer Vision*, 18(3):209–230, 1994.

[60] L. E. Wixson. *Gaze Selection for Visual Search.* PhD thesis, Department of Computer Science, University of Rochester, 1994.

[61] Y. Ye. *Sensor planning in 3D object search.* PhD thesis, Department of Computer Science, University of Toronto, Toronto, Ontario, Canada M5S 1A4, 1996.

[62] Y. Ye and J. K. Tsotsos. The detection function in object search. In *Proceedings of the fourth international conference for young computer scientist*, pages 868–873, Beijing, 1995.

[63] Y. Ye and J. K. Tsotsos. Where to look next in 3d object search. In *1995 IEEE International Symposium for Computer Vision*, Florida, U.S.A, November 19-21 1995.

[64] Y. Ye and J. K. Tsotsos. Sensor planning in 3d object search: its formulation and complexity. In *The 4th International Symposium on Artificial Intelligence and Mathematics*, Florida, U.S.A, January 3-5 1996.

[65] S. Yi. Automatic sensor and light source positioning for machine vision. In *10th International Conference on Pattern Recognition*, pages 55–59, New Jersey, USA, June 1990.

[66] J. Zheng, F. Kishino, Q. Chen, and S. Tsuji. Active camera controlling for manipulation. In *Proc. Computer Vision and Pattern Recognition*, Washington, 1991.

[6] [34] [23] [20] [21] [50] [53] [49] [41] [55] [46] [10] [43] [40] [37] [66] [8] [35] [58] [13] [65] [45] [28] [9] [17] [44] [16] [4] [1] [2] [29] [30] [5] [56] [11] [7] [27] [31] [42] [51] [52] [50] [58] [57] [63] [3]